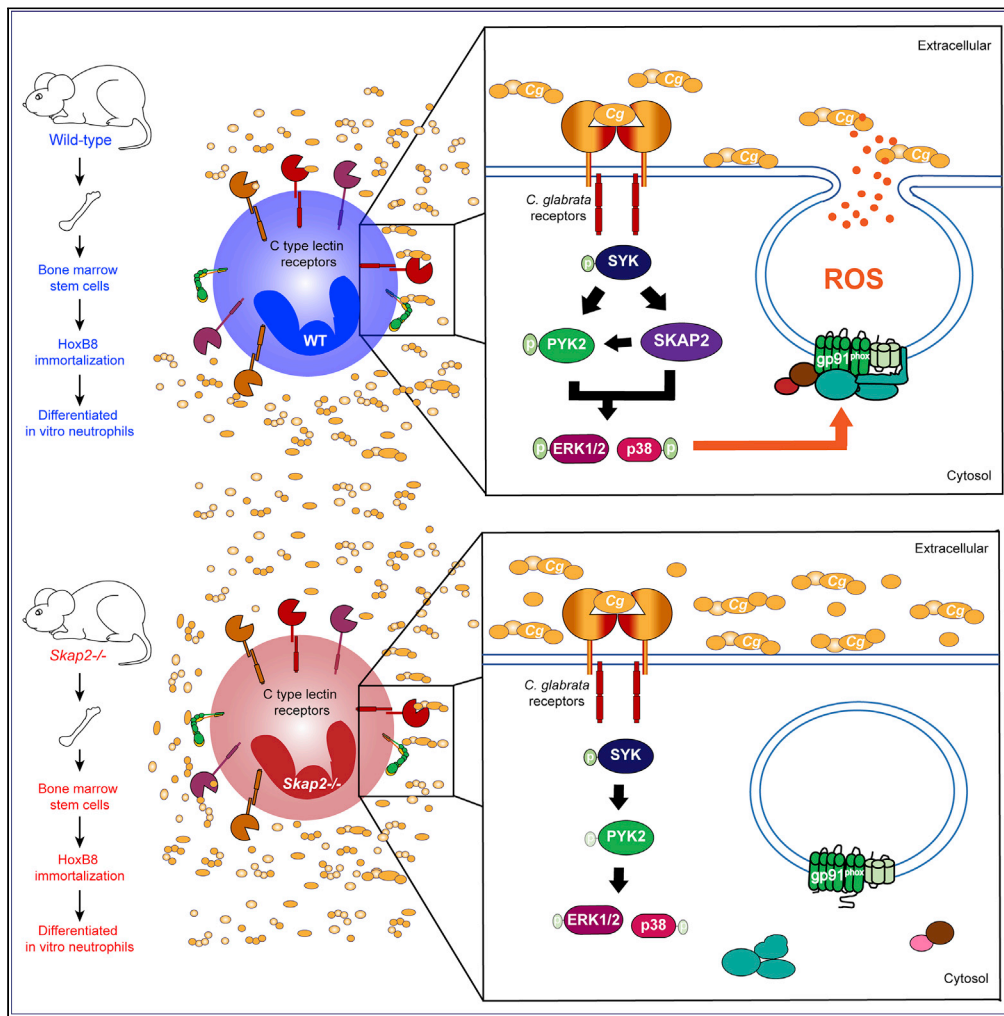


Article

Neutrophils require SKAP2 for reactive oxygen species production following C-type lectin and *Candida* stimulation



Giang T. Nguyen,
Shuying Xu,
Walter Adams, ...,
Michael K.
Mansour, David B.
Sykes, Joan
Mecas

joan.mecas@tufts.edu

Highlights
SKAP-2 regulates
neutrophil ROS following
C-type lectin stimulation

SKAP-2 is required for
C. glabrata-stimulated
neutrophil ROS and killing

Candida and *Klebsiella*-
induced activation of
Pyk2, pERK1/2, and p38
requires SKAP-2

Neutrophils require SKAP-
2 to control
K. pneumoniae infection

Nguyen et al., iScience 24,
102871
August 20, 2021 © 2021 The
Authors.
[https://doi.org/10.1016/
j.isci.2021.102871](https://doi.org/10.1016/j.isci.2021.102871)



Article

Neutrophils require SKAP2 for reactive oxygen species production following C-type lectin and *Candida* stimulation

Giang T. Nguyen,^{1,9} Shuying Xu,^{2,10} Walter Adams,^{3,11} John M. Leong,^{1,3} Stephen C. Bunnell,^{1,4} Michael K. Mansour,^{2,5,6} David B. Sykes,^{5,6,7,8} and Joan Meccas^{1,3,12,*}

SUMMARY

Signaling cascades converting the recognition of pathogens to efficient inflammatory responses by neutrophils are critical for host survival. SKAP2, an adaptor protein, is required for reactive oxygen species (ROS) generation following neutrophil stimulation by integrins, formyl peptide receptors, and for host defense against the Gram-negative bacterial pathogens, *Klebsiella pneumoniae* and *Yersinia pseudotuberculosis*. Using neutrophils from murine HoxB8-immortalized progenitors, we show that SKAP2 in neutrophils is crucial for maximal ROS response to purified C-type lectin receptor agonists and to the fungal pathogens, *Candida glabrata* and *Candida albicans*, and for robust killing of *C. glabrata*. Inside-out signaling to integrin and Syk phosphorylation occurred independently of SKAP2 after *Candida* infection. However, Pyk2, ERK1/2, and p38 phosphorylation were significantly reduced after infection with *C. glabrata* and *K. pneumoniae* in *Skap2*^{-/-} neutrophils. These data demonstrate the importance of SKAP2 in ROS generation and host defense beyond antibacterial immunity to include CLR and *Candida* species.

INTRODUCTION

Neutrophil inflammatory responses to infection are mediated by tyrosine kinase signaling cascades downstream of various pattern recognition receptors, including C-type lectin receptors (CLR), which are critical for host survival (Nguyen et al., 2017). The engagement of CLR, Dectin-1, Dectin-2, or Mincle to bacterial and fungal pathogens, including *K. pneumoniae*, and *Candida* species, results in a diverse repertoire of antimicrobial functions in dendritic cells, macrophages, and neutrophils, including the generation of Dectin-1-mediated NADPH complex-derived reactive oxygen species (ROS) by neutrophils (Sharma et al., 2014, 2017; Li et al., 2011; Wu et al., 2019; Thompson et al., 2019; Netea et al., 2015; Wells et al., 2008; Ifrim et al., 2014; Mansour et al., 2013; Hopke et al., 2020). Dectin-1 binds to β 1,3-glucans, while Dectin-2 and Mincle bind to mannosylated ligands (Dambuzza and Brown, 2015). CLR functions are regulated extensively by expression levels, localization, cooperation through heterodimerization, and crosstalk to β 2 integrins (Ostrop and Lang, 2017; Lee et al., 2012; Li et al., 2011). Functional and biochemical analyses of CLR in dendritic cells and macrophages have shown that their downstream signaling cascades involve the recruitment and phosphorylation of spleen tyrosine kinases (Syk) resulting in such antimicrobial functions, including the release of ROS and pro-inflammatory cytokines to mediate innate and adaptive immune responses (Strasser et al., 2012; Ostrop et al., 2015; Rogers et al., 2005; Yamasaki et al., 2008; Saijo et al., 2010; Negoro et al., 2020).

Neutrophil ROS production is driven by signal transduction pathways downstream of several receptors, including integrin, Dectin-1, Fc γ , and G-protein-coupled receptors (GPCRs), that activate the components of the NADPH oxidase complex (Nguyen et al., 2017). Recently, we and others reported that Src Kinase Associated Phosphoprotein-2 (SKAP2) was essential for ROS production in response to stimulation by integrin and GPCRs, as well as gram-negative bacteria *K. pneumoniae* and *Yersinia pseudotuberculosis* (Nguyen et al., 2020; Shaban et al., 2020; Boras et al., 2017). In addition, SKAP2 is critical for integrin-stimulated cytoskeletal changes in macrophages and neutrophils (Alenghat et al., 2012; Tanaka et al., 2016; Boras et al., 2017). Curiously, while SKAP2 is required for *K. pneumoniae*-mediated Syk phosphorylation in neutrophils (Nguyen et al., 2020), it is not required for integrin or *Y. pseudotuberculosis*-mediated Syk

¹Graduate Program in Immunology, Tufts Graduate School of Biomedical Sciences, Boston, MA 02111, USA

²Division of Infectious Diseases, Massachusetts General Hospital, Boston, MA 02114, USA

³Department of Molecular Biology and Microbiology, School of Medicine, Tufts University, Boston, MA 02111, USA

⁴Department of Immunology, School of Medicine, Tufts University, Boston, MA 02111, USA

⁵Department of Medicine, Massachusetts General Hospital, Boston, MA 02114, USA

⁶Harvard Medical School, Boston, MA 02115, USA

⁷Center for Regenerative Medicine, Massachusetts General Hospital, Boston, MA 02114, USA

⁸Harvard Stem Cell Institute, Cambridge, MA 02115, USA

⁹Present address: Novartis Institutes for BioMedical Research (NIBR), Cambridge, MA 02139, USA

¹⁰Present address: Graduate Program in Immunology, Tufts Graduate School of Biomedical Sciences, Boston, MA 02111, USA

¹¹Present address: Department of Biological Sciences, San Jose State University, San Jose, CA, USA

¹²Lead contact

*Correspondence: joan.meccas@tufts.edu
<https://doi.org/10.1016/j.isci.2021.102871>



phosphorylation in neutrophils (Shaban et al., 2020). Further highlighting the role of SKAP2 in the innate immune response, *Skap2*^{-/-} mice are more susceptible to *K. pneumoniae*, exhibiting a higher *K. pneumoniae* bacterial burden than wild-type controls (Nguyen et al., 2020) and SKAP2 is an essential target of the virulence factor, YopH, in neutrophils during *Y. pseudotuberculosis* infection (Shaban et al., 2020). However, no one has investigated the role of SKAP2 in the activation of neutrophil antimicrobial functions downstream of the CLR family of pattern recognition receptors or fungal infections.

Here, we show that SKAP2 plays a critical role in pathogen recognition by three CLRs, and that SKAP2 is critical for neutrophilic fungicidal response. SKAP2, Src family kinases, and Btk were required for maximal ROS production following stimulation by *C. glabrata*, a fungal species that contributes to 27% of *Candida* bloodstream infections in the US and is increasingly resistant to antifungal agents (Silva et al., 2012; Prevention, 2019). In addition, we identified mitogen-activated protein kinases ERK1/2 and p38 as part of the signaling cascades in neutrophils following the binding of *C. glabrata* and *K. pneumoniae*, and that optimal phosphorylation of ERK1/2 and p38 requires SKAP2. This study demonstrates and extends the importance of *Skap2* in host defense to an additional microbial kingdom and highlights the need to investigate the role of *Skap2* in human disease.

RESULTS

Transferred HoxB8-derived *Skap2*^{-/-} neutrophils fail to control *K. pneumoniae* infection in neutrophil-depleted mice

To aid our studies of neutrophil functions, we used a granulocyte-monocyte progenitor (GMP) cell line that was conditionally immortalized by the enforced expression of an estrogen receptor-homeobox B8 (ER-Hoxb8) as previously described (Sykes and Kamps, 2001; Saul et al., 2019; Nguyen et al., 2020) (see STAR Methods). The media for these cells contains stem cell factor and estradiol (E2), which permits nuclear translocation of ER-Hoxb8 fusion protein, resulting in the conditional maturation arrest at the GMP stage. The removal of E2 from the cell media, coupled with interleukin-3 (IL-3) and granulocyte colony stimulating factor (G-CSF) permits synchronous differentiation of GMP into mature neutrophils, which we termed differentiated *in vitro* (DIV) neutrophils (Nguyen et al., 2020). BALB/c wild-type and *Skap2*^{-/-} DIV neutrophils were previously characterized and shown to be morphologically and functionally similar to their bone marrow (BM) counterparts (Nguyen et al., 2020).

DIV neutrophils derived from C57BL/6J (B6) mice are morphologically and functionally similar to their BM counterparts *in vitro* (Negoro et al., 2020; Chu et al., 2019). However, unlike the DIV derived from mice on a BALB/c background, DIV neutrophils generated from the B6 background do not express Ly6G homodimers on their surface, and only Gr-1 (Ly6G-Ly6C heterodimers) (Figure S1). To evaluate whether DIV neutrophils are functional *in vivo*, B6 wild-type and B6 *Skap2*^{-/-} DIV neutrophils were transfused into neutropenic B6 mice generated by injection of α -Ly6G (clone: 1A8), followed by intranasal infection with *K. pneumoniae* (ATCC 43816). Consistent with prior studies (Xiong et al., 2015; Nguyen et al., 2020; Ye et al., 2001), *K. pneumoniae* reached between 10^5 - 10^6 colony forming units (cfu) in wild-type (Figure 1A, control, black circles) and in neutropenic mice that received B6 wild-type DIV (Figure 1A, blue triangles) by 24 hours post-infection. However, mice that received B6 *Skap2*^{-/-} DIV neutrophils (Figure 1A, red triangles) yielded a significantly higher bacterial burden with 10^7 cfu on average. The bacterial burden observed in neutropenic mice that received B6 DIV neutrophils (Figure 1A, blue triangles) was similar to what we previously observed in irradiated BALB/c mice that received wild-type BM cells that were depleted of inflammatory monocytes (Nguyen et al., 2020). This data indicates that *Skap2*-expressing DIV neutrophils are functionally comparable to BM-derived *Skap2*-expressing neutrophils *in vivo* in controlling bacterial burden, and that SKAP2-mediated neutrophil effector functions are critical for host protection against *K. pneumoniae* pneumonic infection. Further, by taking advantage of the lack of Ly6G expression on B6 DIV neutrophils, we can selectively deplete the host's neutrophils without irradiation treatments, which keeps the rest of the immune system intact while allowing us to dissect the molecular mechanisms controlling neutrophil functions *in vivo* using HoxB8-derived neutrophils.

Skap2 in neutrophils is dispensable for the expression of Mincle, Dectin-2, Dectin-1, and integrin receptors during pneumonic *K. pneumoniae* infection

Neutrophils from *K. pneumoniae*-infected lungs were previously shown to express Mincle receptors, which are critical for host defense and neutrophil function against *K. pneumoniae* (ATCC 43816) (Sharma et al., 2014, 2017). To determine if other CLRs are potentially playing a role in the pathogenesis of *K. pneumoniae* pneumonia, we surveyed the expression of Dectin-2 and Dectin-1 in the lungs of mice by flow cytometry (Figure S2). Consistent with prior data (Sharma et al., 2014), 99% of the highly

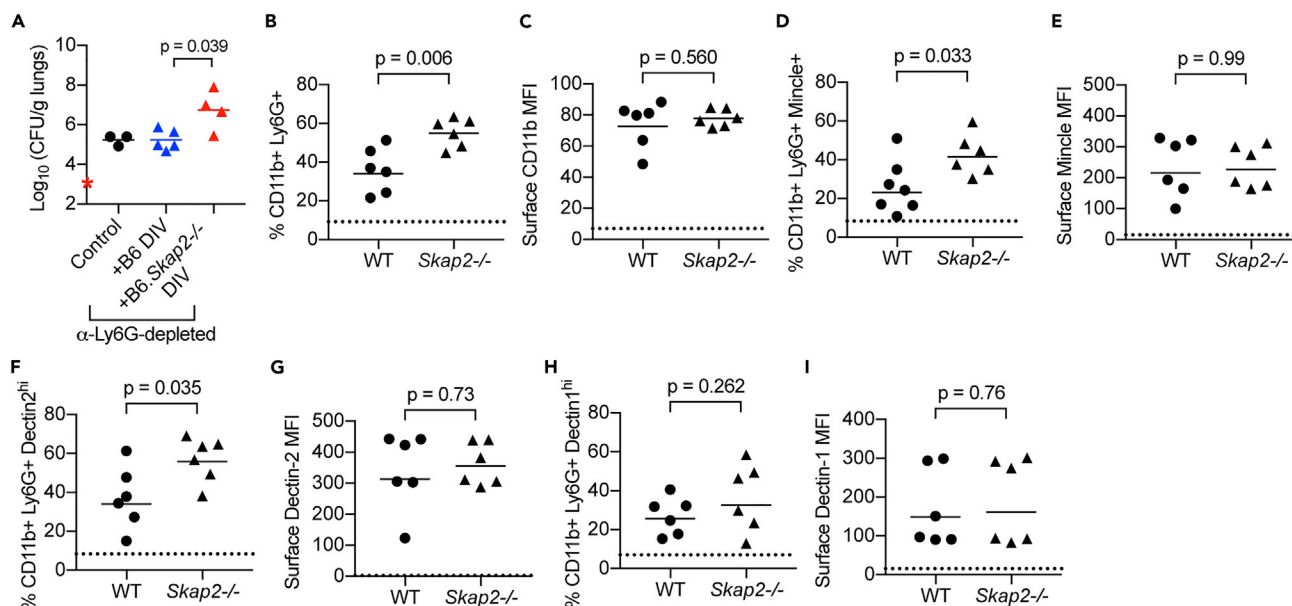


Figure 1. Transferred *Skap2*^{-/-} DIV neutrophils fail to control *K. pneumoniae* infection in neutrophil-depleted mice despite normal C-type lectin receptor expression

(A) C57BL/6J (B6) wild-type mice were treated with PBS (control, black circles) or α -Ly6G (1A8, triangles) antibody intraperitoneally. 16 hours post-antibody injection, α -Ly6G-treated mice were intravenously injected with sterile PBS containing no cells (black triangles), B6 wild-type (blue triangles) and *Skap2*^{-/-} (red triangles) DIV neutrophils (see STAR Methods). All B6 mice were then infected retropharyngeally with 5×10^3 cfu *K. pneumoniae*. Lungs were harvested after 24 hours and plated for bacterial burden (log (cfu/g lungs)). Data were compiled from $n = 3$ independent experiments with 1–3 mice each group. (B–I) BALB/c wild-type (WT) or *Skap2*^{-/-} mice were infected intranasally with *K. pneumoniae*, and lungs were harvested after 24 hours. Cells were stained with CD11b and Ly6G, fixed with 4% formaldehyde, and stained with α -Dectin-1, α -Mincle, or α -Dectin-2 along with their respective secondary fluorescent-conjugated antibody (see STAR Methods). Neutrophils (CD11b⁺ Ly6G⁺) were further gated to analyze expression of Dectin-1, Mincle, and Dectin-2. CD11b + Ly6G + cells were assessed for CLR and CD11b integrin expression, and presented as (B, D, F, and H) percent of cells, or (C, E, G, and I) mean fluorescent intensity (MFI). Data are compiled from $n = 2$ independent experiments with 3 mice each group. Center bars are geometric means, and each dot represents a mouse. Dotted lines indicate (B, D, F, and H) average level in PBS-treated lungs or (C, E, G, and I) MFI of sample stained with fluorescent-conjugated secondary antibody only. Significance was assessed using (A) one-way ANOVA with Sidak's, or (B–I) two-tail unpaired Student's *t* test. See also Figures S1 and S2.

Mincle-positive cells in the lungs of *K. pneumoniae* infected mice were CD11b⁺ Ly6G⁺ neutrophils (Figure S2A). In addition, flow cytometry showed lung cells expressing variable levels of Dectin-2 and Dectin-1, with the majority of cells that expressed high levels of Dectin-1 and Dectin-2 being CD11b⁺ Ly6G⁺ neutrophils (Figures S2B and S2C). These data show that Mincle, Dectin-1, and Dectin-2 are expressed on neutrophils, and may play a role in the pathogenesis of *K. pneumoniae* pneumonia. We next evaluated if the increased susceptibility of *Skap2*^{-/-} mice to *K. pneumoniae* infection (Figure S2D) was due to differences in the expression of CLR on neutrophils in *K. pneumoniae*-infected BALB/c wild-type (WT) and *Skap2*^{-/-} lungs. Although there were more neutrophils recovered from *K. pneumoniae*-infected *Skap2*^{-/-} lungs than WT lungs, there was no difference in the surface expression of CD11b (Figures 1B, 1C, and S2E), consistent with our prior DIV neutrophil data (Nguyen et al., 2020). Higher numbers of Mincle- and Dectin-2-positive cells and equivalent numbers of Dectin-1 expressing cells were recovered from *K. pneumoniae*-infected *Skap2*^{-/-} lungs (Figures 1D–1I and S2F–S2H). Collectively, these data show the CLR are present on surfaces of neutrophils during *K. pneumoniae* infection independent of the presence of SKAP2, so the increased bacterial burden observed in *Skap2*^{-/-} mice was likely not due to the lack of these receptors.

SKAP2 modulates the activation of ROS production downstream of TDB, furfuran, and curdlan stimulation

ROS is required for host protection against *K. pneumoniae*. Patients with chronic granulomatous disease generate less ROS than healthy hosts, and are highly susceptible to life-threatening *K. pneumoniae* respiratory infections (Bortoletto et al., 2015; Wolach et al., 2017), while ROS defective mice (B6-Cybb^{-/-}) suffer from higher bacterial burdens than B6 mice (Nguyen et al., 2020; Paczosa et al., 2020). We examined

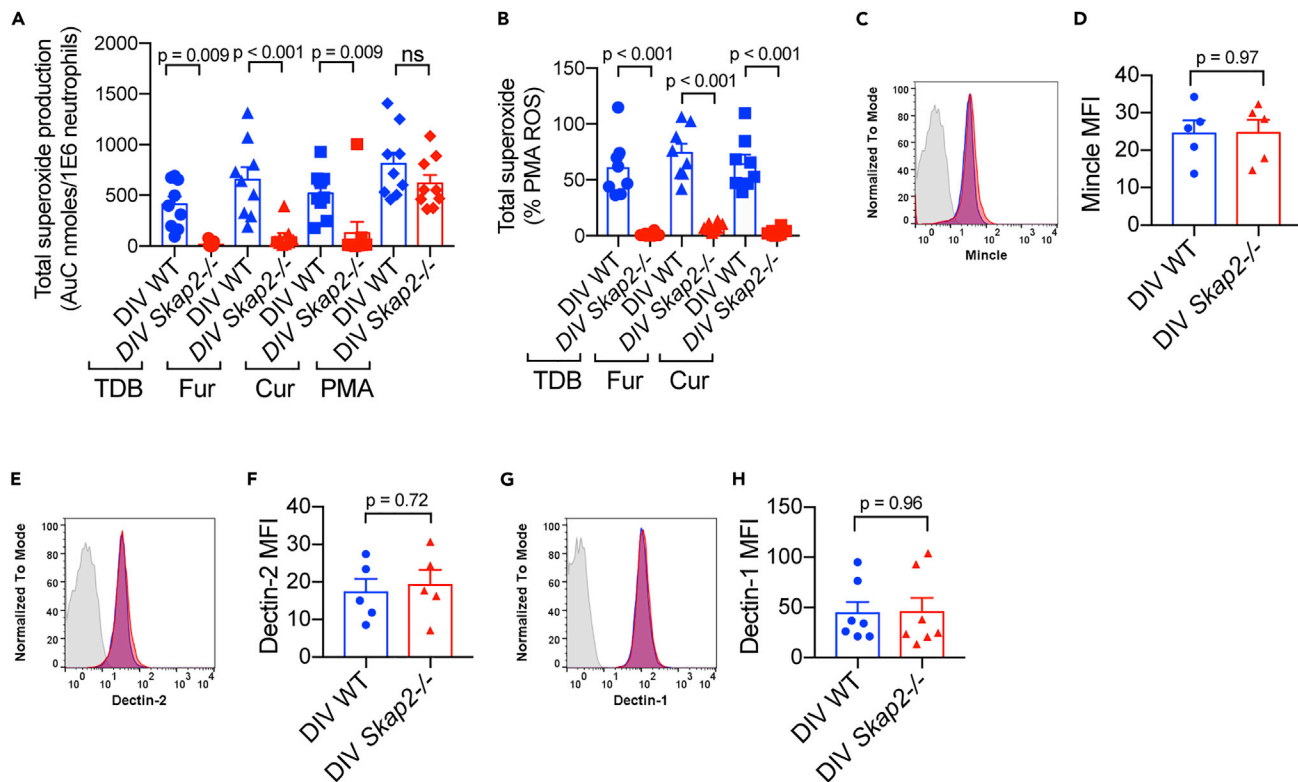


Figure 2. TDB, furfuran, and curdian-induced ROS requires SKAP2

(A and B) The respiratory burst of BALB/c wild-type (WT) and *Skap2*^{-/-} DIV neutrophils plated on immobilized TDB, an agonist for mincle-containing dimers, furfuran (Fur), an agonist for Dectin-2, or curdian (Cur), an agonist to Dectin-1. The total concentration of superoxide produced after 60 min was calculated by the sum of the area under the curves and presented as (A) total superoxide (values were normalized to unstimulated samples of each respective genotype), or (B) as percentage of PMA-induced ROS. Data are presented as mean \pm SEM compiled from n = 8–9 independent experiments from two different HoxB8-GMP cell lines per each genetic background (WT or *Skap2*^{-/-}).

(C–H) DIV neutrophils were stained with CD11b and Ly6G, fixed with 4% formaldehyde, and stained with α -Mincle, α -Dectin-2, or α -Dectin-1. Surface receptor levels are reported as mean fluorescence intensity (MFI) with mean \pm SEM from n = 5–7 independent experiments from two different HoxB8-GMP cell lines. Significance was assessed using (A and B) one-way ANOVA with Sidak's, or (D, F, and H) two-tail unpaired Student's t test.

See also Figure S3.

whether *Skap2*^{-/-} neutrophils are defective for ROS production following stimulation with the purified ligands trehalose-6,6'-dibehenate (TDB), furfuran, or curdian, which stimulate Mincle homo/heterodimers, Dectin-2 and Dectin-1 homodimers, respectively. A cytochrome c absorbance assay was used to detect superoxide production (Nguyen et al., 2020; Dahlgren et al., 2020; Shaban et al., 2020). DIV and BM BALB/c wild-type (WT) neutrophils stimulated with TDB, furfuran, or curdian produced significantly higher levels of superoxide compared with *Skap2*^{-/-} counterparts (Figures 2A, 2B, and S3). The loss in ROS production was not due to defects in NADPH oxidase as *Skap2*^{-/-} BM and DIV neutrophils robustly released ROS following PMA stimulation (Figure 2A), or to changes in the expression of Mincle, Dectin-2, and Dectin-1 on the surface of *Skap2*^{-/-} DIV neutrophils (Figures 2C–2H).

SKAP2 is required for TDB, furfuran, and curdian-stimulated cell adhesion

CLR activation triggers cell adhesion, spreading, and actin polymerization (Lee et al., 2012, 2017). These processes may influence ROS production, as the regulatory components of the NADPH oxidase complex interact with the actin cytoskeleton in both resting and activated neutrophils (el Benna et al., 1994; Nauseef et al., 1991; Woodman et al., 1991). Therefore, we examined whether SKAP2 is required for neutrophil spreading following TDB, furfuran, and curdian stimulation. After one hour of TDB, furfuran, or curdian stimulation, WT neutrophils adhered strongly to agonist-coated surfaces with 40–60% of the cells spreading to the agonist-coated wells in contrast to cells plated onto unstimulated surfaces (Figures 3A–3D, 3K, and 3L). However, the percentage of *Skap2*^{-/-} neutrophils that spread on CLR agonist-coated surfaces was

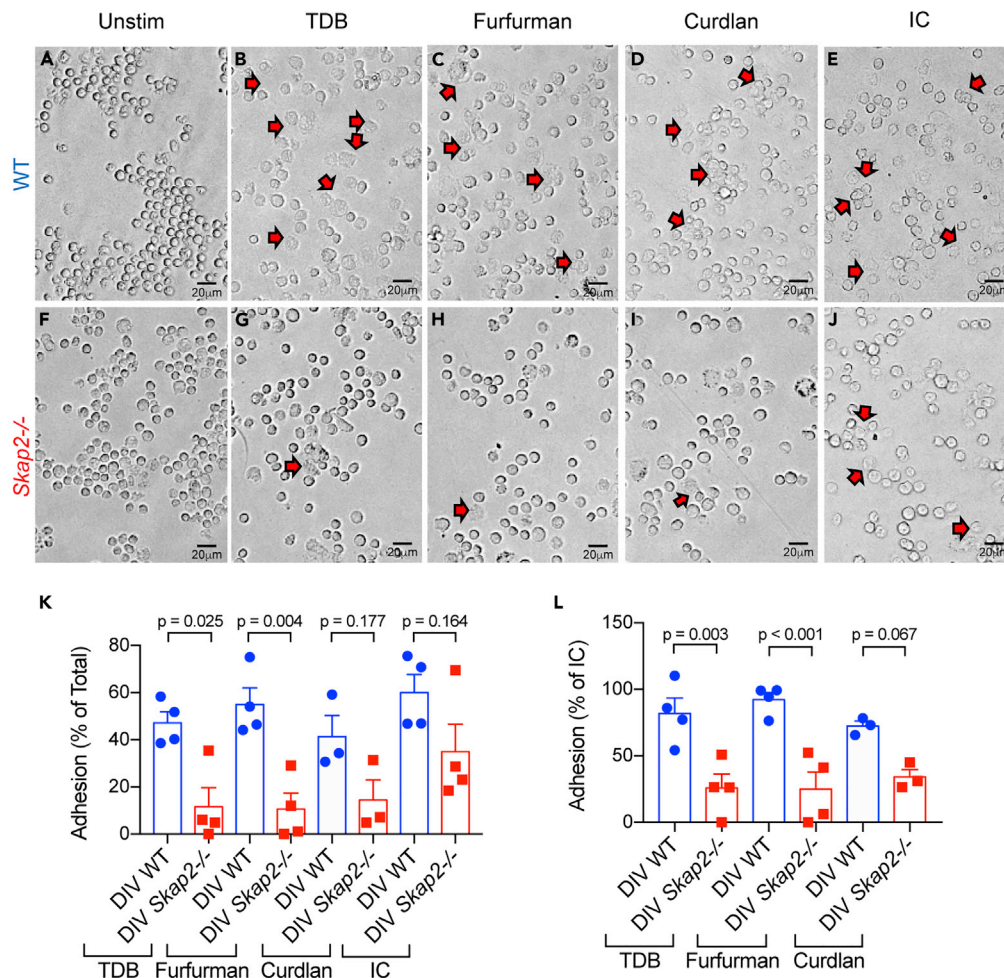


Figure 3. TDB, furfurman, and curdlan-stimulated neutrophil adhesion are SKAP2-dependent

(A–J) Firmly-adherent WT (A–E) and *Skap2*^{-/-} (F–J) DIV neutrophils stimulated with immobilized TDB (B, G), furfurman (C–H), or curdlan (D, I) for 1 hour were imaged by bright-field microscopy. Control cells were plated onto surface coated with 10% FBS (Unstim) (A, F), or IgG immune complexes (IC) (E, J) for 1 hour. Original magnification was 20 \times (n = 3–4 independent experiments in technical duplicates).

(K and L) Images were blinded prior to counting the number of rounded and spread cells, which are presented as the percentage of (K) total cells counted (values were normalized to unstimulated samples of each respective genotype), or (L) of IC-induced adhered neutrophils. Significance was assessed using (K) one-way, or (L) two-way ANOVA with Sidak's post-test.

3- to 4-fold less (Figures 3F–3I, 3K, and 3L). The reduction in cell spreading was not due to global defects in cytoskeletal rearrangement as *Skap2*^{-/-} DIV neutrophils were able to spread on surfaces coated with IgG immune complexes (IC) albeit at only 60% of WT levels (Figures 3E and 3J–3L). The reduced IC-induced spreading observed in *Skap2*^{-/-} neutrophils was consistent with a previously reported reduction in IC-stimulated ROS production (Nguyen et al., 2020; Shaban et al., 2020). These data indicate that SKAP2 plays a role in CLR-induced cytoskeletal rearrangement leading to adhesion, and that the reduction in SKAP2-dependent, CLR-stimulated cytoskeletal remodeling in *Skap2*^{-/-} neutrophils may hinder ROS production.

SKAP2 is not required for TDB, furfurman, or curdlan-stimulated integrin activation

In neutrophils, Dectin-1 activates integrin receptors in response to zymosan, another Dectin-1 agonist, causing β_2 integrins to undergo conformational changes from inactive to high affinity states (Li et al., 2011). High affinity integrin states trigger ROS production and can be assessed by rapid and inducible binding to ligands such as fibrinogen, which binds to β_2 (CD11b/CD18) integrins (Van Strijp et al., 1993; Boras et al., 2017; Fagerholm et al., 2019; Adams et al., 2021). To determine if Mincle and Dectin-2 stimulation also induced an integrin conformational change to the high affinity form in neutrophils, a flow cytometric

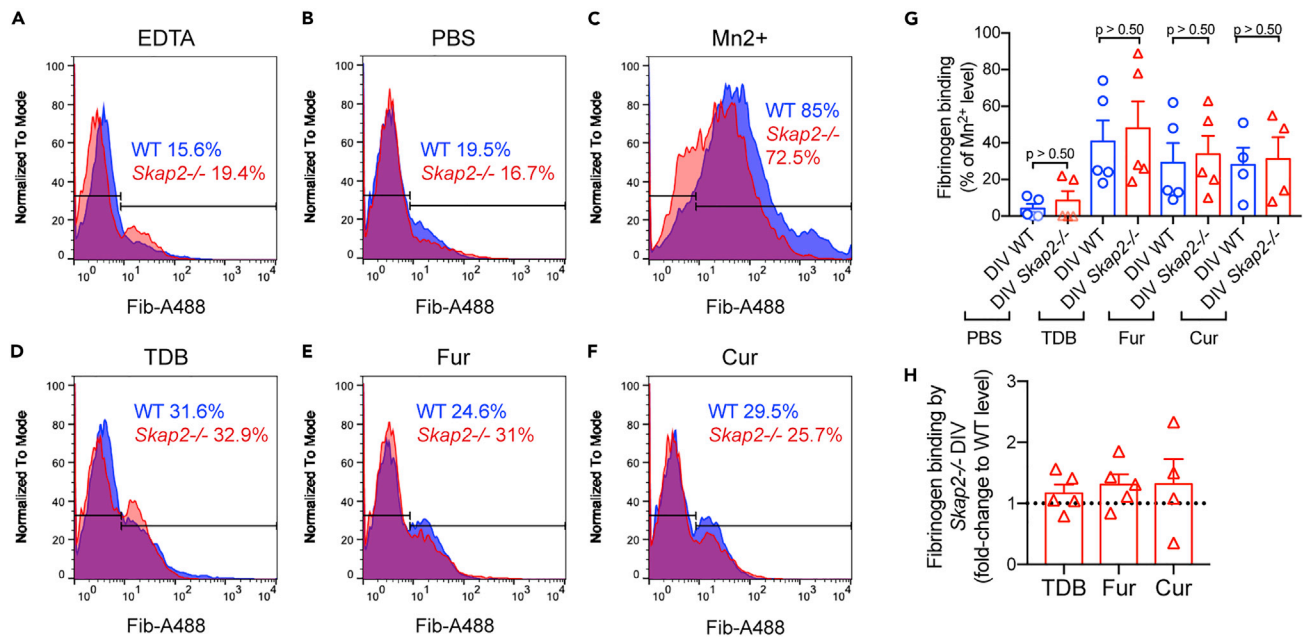


Figure 4. SKAP2 is not required for CLR-induced integrin activation

The assessment of high affinity integrin conformation was measured by the binding of soluble Alexa 488-conjugated fibrinogen to WT and *Skap2*^{-/-} neutrophils stimulated with TDB, furfuran (Fur), and curdlan (Cur). Neutrophils were stimulated for 20 min at 37°C with 5% CO₂. Alexa 488-conjugated fibrinogen was then added to each well, and the cells were incubated for another 15 min at 37°C with 5% CO₂. Some cells were left untreated/unstimulated (PBS), treated with 2.5mM Mn²⁺ as a positive control for the last 15 min of incubation, or treated with 2.5mM EDTA for 30 min prior to the addition of fibrinogen to the plate as negative control. Cell suspensions were collected, fixed with 1% formaldehyde, and analyzed by flow cytometry.

(A–F) Representative histograms gated on live cells.

(G) The quantification of the percentage of fibrinogen-bound cells by DIV neutrophils (normalized to EDTA-treated level, divided by % of fibrinogen-bound by Mn²⁺-treated cells).

(H) Level of fibrinogen-bound cells by *Skap2*^{-/-} DIV neutrophils as fold-change to WT level. The data are presented as the mean ± SEM from n = 4–5 independent experiments in technical duplicate. Significance was assessed using two-way ANOVA with Sidak’s post-test.

binding assay with Alexa 488-conjugated fibrinogen was used (Figures 4A–4F). About 60–80% of murine neutrophils bound fibrinogen following treatment with Mn²⁺, the positive control for integrin activation (Figure 4C) (Dransfield et al., 1992; Ye et al., 2012). TDB, furfuran, or curdlan treatment of WT neutrophils resulted in integrin activation at approximately 40%, 30%, and 30% of Mn²⁺ level, respectively (Figures 4D–4G). To determine whether SKAP2 is required to induce integrin conformational changes, we assessed whether *Skap2*^{-/-} neutrophils had defects in CLR-induced integrin activation. We observed that similar percentages of *Skap2*^{-/-} DIV neutrophils bound to Alexa 488-conjugated fibrinogen following TDB, furfuran, or curdlan stimulation indicating that CLR-induced integrin conformational changes are not SKAP2-dependent (Figures 4D–4H). Combined, these data suggest that SKAP2-dependent defects in ROS are due to deficiencies in the signaling cascades downstream of CLRs or integrins rather than changes in integrin activation.

SKAP2 is required for maximal *C. glabrata* and *C. albicans*-stimulated ROS production and overall fungal killing

Dectin-1, Dectin-2, Mincl, and β2 integrin receptors have all been individually proposed to be critical for fungal resistance in mice and humans (Chen et al., 2017; Feinberg et al., 2017; Ifrim et al., 2014; Sato et al., 2006; Wu et al., 2019; Saijo et al., 2010; McGreal et al., 2006; Zhu et al., 2013; Brown et al., 2003; Taylor et al., 2007; Ferwerda et al., 2009). The leading cause of invasive fungal infections involves *Candida* species including the morphologically and genetically different species, *C. albicans* and *C. glabrata*, that together account for 50–90% of cases in North America and Europe with a 40–50% mortality rate (Arendrup et al., 2011; Tortorano et al., 2006; Prevention, 2019). These three CLRs contribute to *C. albicans*-induced neutrophil ROS production and are critical for the clearance of *C. albicans* (Thompson et al., 2019). Dectin-1

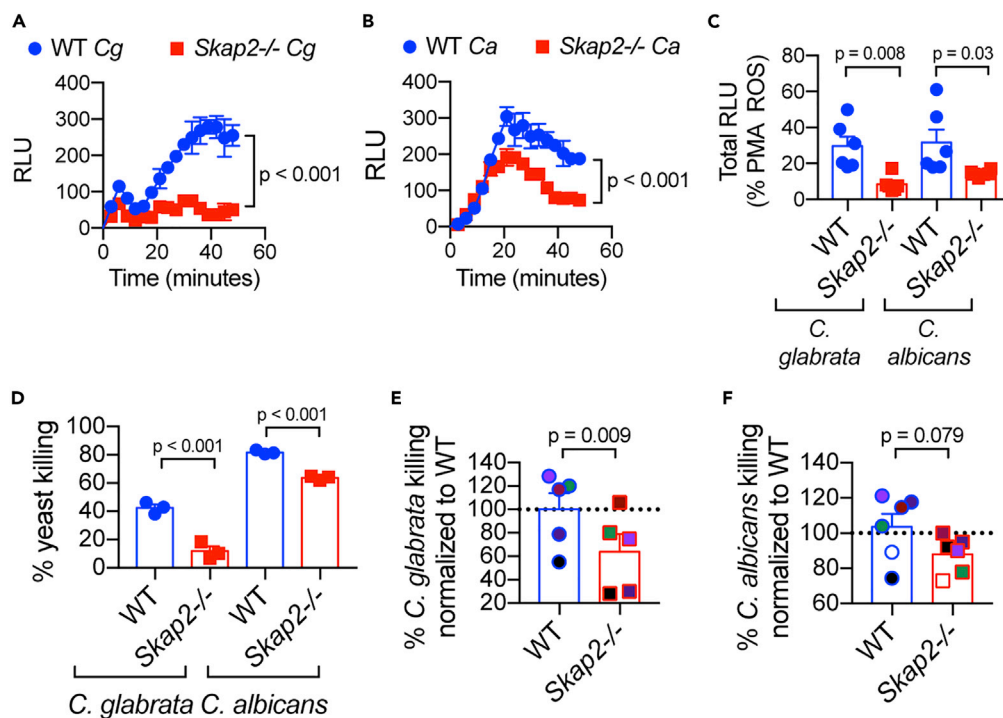


Figure 5. SKAP2 is required for maximal *C. glabrata* and *C. albicans*-induced ROS production, and neutrophil killing

(A–C) The respiratory burst of WT and *Skap2*^{−/−} DIV neutrophils following *C. glabrata* and *C. albicans* stimulation (MOI 1) using isoluminol chemiluminescence. (A and B) A representative experiment performed in technical triplicate with data presented as mean ± SEM. Values shown are with background subtraction of the unstimulated samples plated on FBS-coated surface. (C) The total concentration of superoxide produced after 45 min was calculated by the sum of the area under the curves and presented as the percentage of PMA-induced ROS. DIV data are presented as mean ± SEM compiled from n = 6 independent experiments in technical triplicates. Significance was assessed using two-way ANOVA with (A and B) Tukey’s post-test or (C) Sidak’s post-test.

(D–F) WT and *Skap2*^{−/−} DIV neutrophils were co-incubated with yeasts (*C. albicans* for 2 hr, and *C. glabrata* for 18 hr) at MOI 0.2. Neutrophils were lysed and PrestoBlue dye was then added to measure the yeast viability by fluorescent readings. Percent of yeast killing was calculated as follows: 100 – (100*viability of yeast plus neutrophils/viability of yeast only). (D) Data are a representative in technical triplicate, and significance was assessed using two-way ANOVA with Sidak’s. (E and F) The average yeast killing of technical replicates was calculated from each independent experiment. The *Skap2*^{−/−} values were divided by WT values in each respective experiment. The WT level of yeast killing in each experiment was set to 100 as indicated by the dotted line. The percent of yeast killing by WT DIV neutrophils was divided by the average of the 5–6 experiments. Data were compiled from n = 5–6 independent experiments and presented as mean ± SEM with each experiment represented by a different color. Significance was assessed using paired Student’s t-test.

engagement leads to the activation of integrin receptors, resulting in neutrophil ROS production and protection against systemic *C. albicans* infection in mice (Li et al., 2011).

To dissect the contribution of SKAP2 in *C. glabrata* and *C. albicans*-activated neutrophils, the ROS production by *Skap2*^{−/−} DIV neutrophils was assessed using isoluminol chemiluminescence (Nguyen et al., 2020; Dahlgren et al., 2020; Shaban et al., 2020). When stimulated with *C. glabrata* and *C. albicans*, WT DIVs generated robust and persistent ROS while *Skap2*^{−/−} DIVs generated 50% and 25% of the levels produced by WT DIVs, respectively (Figures 5A–5C). Next, we examined whether the defects in ROS affected the fungal killing ability by *Skap2*^{−/−} DIV neutrophils. DIV neutrophils were incubated with *C. glabrata* for 24 h, or *C. albicans* for 2 h, and then fungal survival was measured using the PrestoBlue viability dye conversion (Xu et al., 2018; Tam et al., 2019). Compared to WT, *Skap2*^{−/−} DIV neutrophils demonstrated significantly decreased fungicidal activity after infection with *C. glabrata* (Figures 5D and 5E), while infection with *C. albicans* typically also led to a decrease in fungal killing in 4 out of 5 experiments (Figures 5D and 5F).

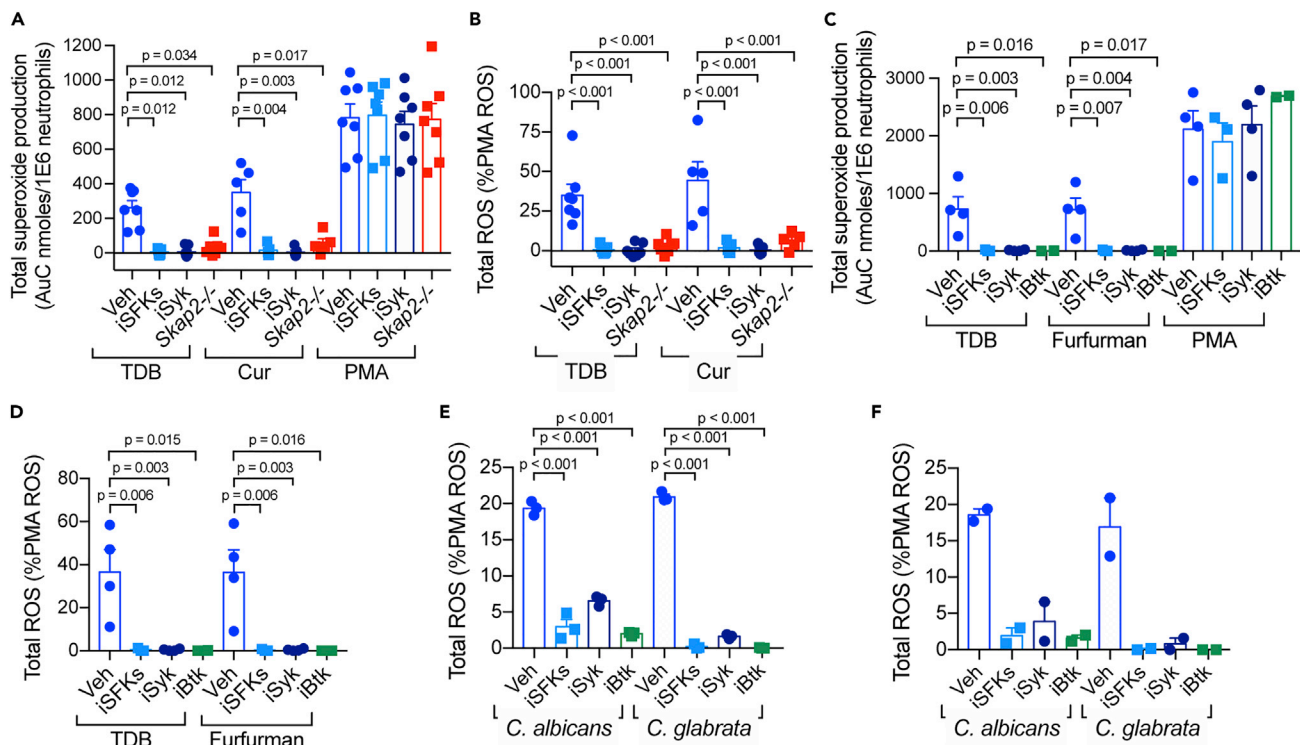


Figure 6. SFK-Syk-Btk are required for neutrophil ROS production following stimulation of TDB, curdlan, furfuran, *C. albicans*, and *C. glabrata*

The respiratory burst of DIV (A, B, E, and F) or human (C and D) neutrophils treated with inhibitors using (A–D) a cytochrome C assay or (E and F) isoluminol chemiluminescence. (A–D) Neutrophils were pre-treated with DMSO (Veh), PP2 (iSFKs), R406 (iSyk), or Ibrutinib (iBtk) for 10 min at 37°C and then plated onto immobilized TDB, furfuran, or curdlan (cur), and measured for 60 min. (E and F) DIV neutrophils were pre-treated with inhibitors as in (A–D), and then infected with *C. albicans* or *C. glabrata* (MOI 1) and measured for 30 min. (E) A representative experiment is shown in technical triplicate with data presented as mean \pm SEM. The total superoxide was calculated as area under the curve after subtracting the uninfected samples, and presented as (A and C) total production or (B) as percentage of PMA-induced ROS. (A–D and F) Data are compiled from (B–D) $n = 4$ –7 or (F) $n = 2$ independent experiments performed in technical triplicate and presented as mean \pm SEM with dots representing averages of independent experiments. Significance was assessed using one-way ANOVA with Sidak's post-test.

Combined, these data indicate that the SKAP2 deficiency resulted in an abrogated neutrophil ROS production after infection with *C. glabrata* and *C. albicans* that potentially enables fungal escape with *C. glabrata* appearing more sensitive to SKAP2-mediated responses.

SFKs-Syk-Btk are required for neutrophil ROS production following stimulation of TDB, curdlan, furfuran, *C. albicans*, and *C. glabrata*

Previous studies demonstrate Syk involvement in neutrophil ROS production in response to stimulation by Dectin-1 agonists, *C. albicans*, and *C. glabrata* (Deng et al., 2015; Negoro et al., 2020; Li et al., 2011). Consistent with these data, pretreatment of WT DIV with a small molecule inhibitor of Syk, R406, produced significantly lower TDB-stimulated ROS than their vehicle-treated counterpart (Figures 6A and 6B). Likewise, pretreatment of human neutrophils with R406 inhibited TDB- and Furfuran-stimulated ROS production (Figures 6C and 6D). Inhibitors of Src Family Kinases (SFKs), which act upstream of Syk, and of Bruton's Tyrosine Kinase (Btk), which mediates phospholipase C activation downstream of Syk, also inhibited TDB-, Furfuran- and curdlan-induced ROS production (Figures 6A–6D) consistent with prior data in human neutrophils using PP2 (iSFK) and β -glucan beads (Nani et al., 2015). While Btk has been shown to contribute to neutrophil ROS, phagocytosis, and overall mouse survival during *C. albicans* infection (Colado et al., 2020; Strijbis et al., 2013), the role of SFKs and Btk in *C. glabrata* infection is unclear. Here, inhibitors of Syk, SFKs, and Btk also significantly reduced *C. glabrata*- and *C. albicans*-induced ROS production by DIV neutrophils (Figures 6E and 6F), suggesting that in addition to Syk (Negoro et al., 2020) and SKAP2 (Figure 5), *C. glabrata*-stimulated ROS also requires SFKs and Btk.

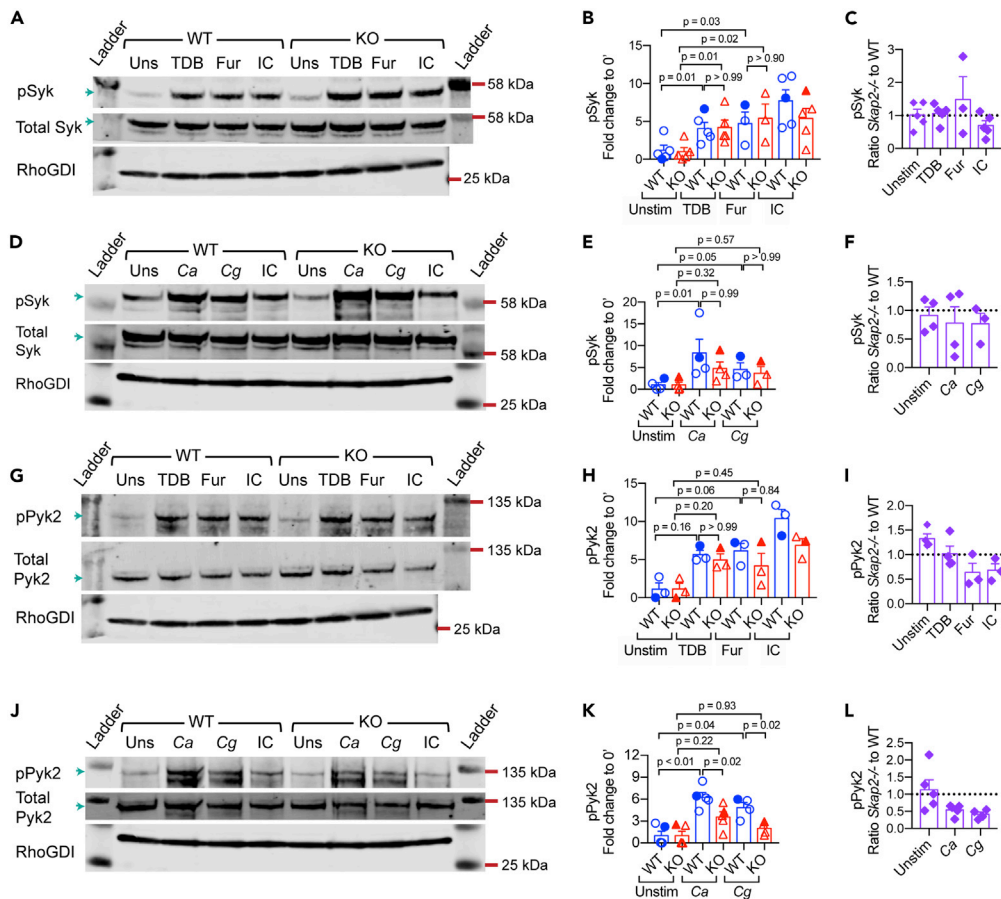


Figure 7. SKAP2 is required for optimal *C. glabrata*-stimulated phosphorylation of Pyk2 but not Syk kinases
 WT and *Skap2*^{-/-} neutrophils were (A–C and G–I) plated onto immobilized TDB, furfuran (Fur), or IgG immune complexes (IC), or (D–F and J–L) stimulated with MOI 2 of *C. albicans* or *C. glabrata* for 15 min at 37°C. Lysates were analyzed by Western blot for pSyk (Y352), pPyk2 (Y402), and RhoGDI, then stripped, and re-probed for respective total proteins. Quantification is shown in Tables S1–S4. Data were compiled from 3–5 independent experiments. (A, D, G, and J) Representative blot shown with arrows to indicate bands used for analysis. (B, E, H, and K) Fold change from each experiment with respect to unstimulated, symbols represent the value from each experiment, solid symbols indicating values of blot shown, bars indicate mean. Statistics represent mean ± SEM. (C, F, I, and L) The *Skap2*^{-/-} values were divided by WT values in each respective experiment. The average WT level of CLR-stimulated phosphorylation was set to 1 as indicated by the dotted line. Data were compiled from n = 3–5 independent experiments with data presented as mean ± SEM. Significance was assessed using (B, E, and H) two-way ANOVA with Tukey’s post-test or (K) one-way ANOVA within each group, or two-way ANOVA between WT and KO groups with Sidak’s post-test. See also Figure S4 and Tables S1–S4.

SKAP2 is required for optimal *C. glabrata*-stimulated phosphorylation of Pyk2, but not Syk, kinases

Previously, we showed that SKAP2 contributes to *K. pneumoniae*-induced activation of tyrosine kinases Syk and Pyk2 (Nguyen et al., 2020), which also function downstream of integrin receptors (Mocsai et al., 2002). To determine whether SKAP2 was required for the phosphorylation of Syk and Pyk2 following TDB, furfuran, or *Candida*-challenged WT and *Skap2*^{-/-} DIV neutrophils were analyzed. Consistent with prior work in BM neutrophils using zymosan, a Dectin-1 agonist (Li et al., 2011), WT DIV neutrophils stimulated with TDB, furfuran, *C. albicans*, and *C. glabrata* enhanced the phosphorylation of Syk and Pyk2 relative to unstimulated controls (Figures 7 and S4A–S4C, Tables S1–S4). However, in contrast to infection with *K. pneumoniae* (Nguyen et al., 2020), the loss of SKAP2 deficiency did not significantly reduce Syk phosphorylation downstream of TDB, furfuran, *C. glabrata* and *C. albicans* stimulation (Figures 7A–7F and S4, Tables S1 and S2), or TDB

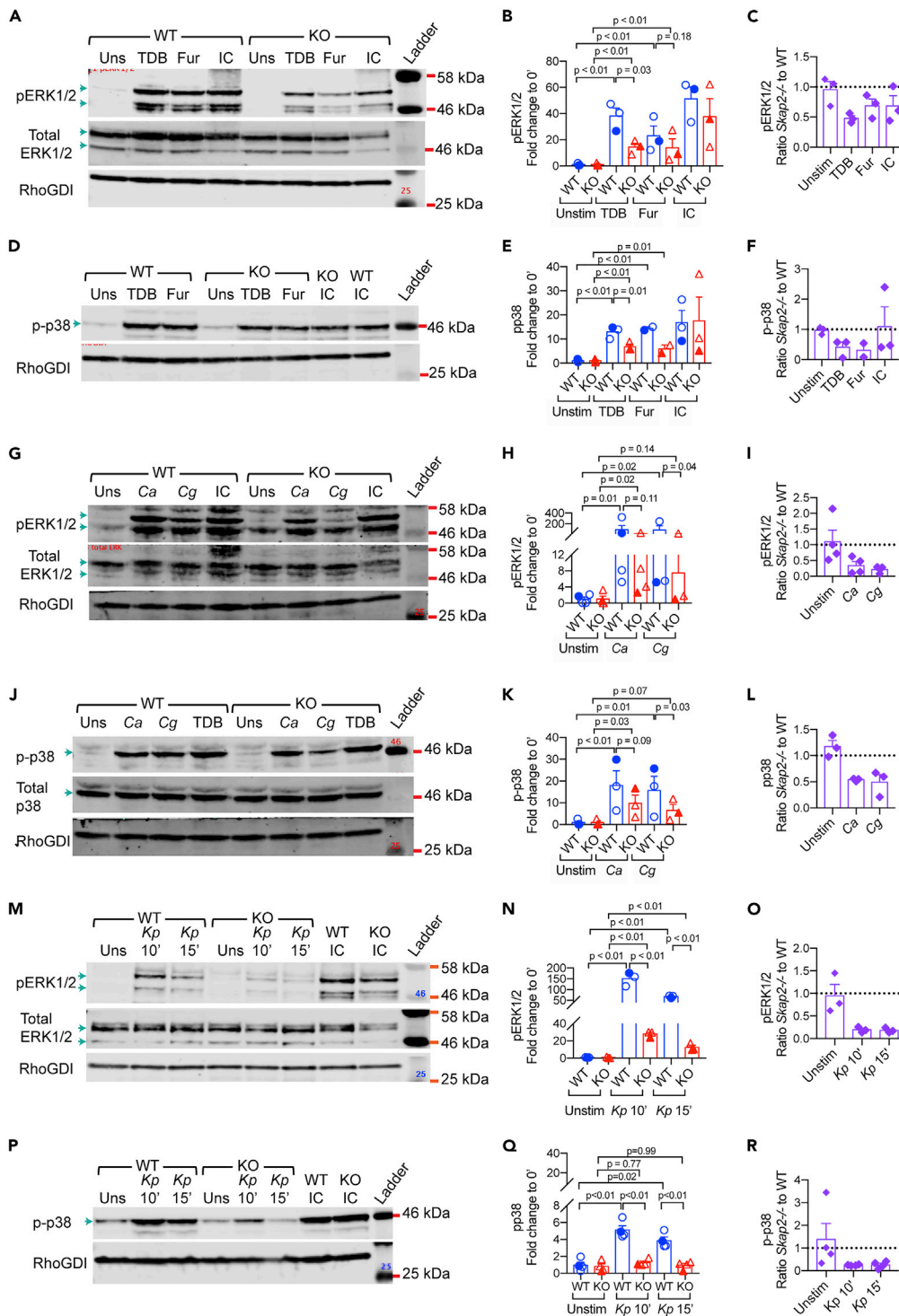


Figure 8. SKAP2 is required for optimal *C. glabrata*, and *K. pneumoniae*-induced ERK1/2 and p38 phosphorylation

WT and *Skap2*^{-/-} neutrophils were (A–F) plated onto immobilized TDB, furfuran (Fur), or IgG immune complexes (IC), or stimulated with (G–L) MOI 2 of *C. albicans* and *C. glabrata* for 15 min or (M–R) MOI 40 of *K. pneumoniae* for 10 or 15 min at 37°C. Lysates were analyzed by Western blot for pERK1/2, p38, and RhoGDI, then stripped, and re-probed for respective total proteins. Quantification was completed as described in Tables S5–S9. (A, D, G, J, M, and P) Representative blot shown with arrow to indicate bands used for analysis. (B, E, H, K, N, and Q) Fold change from each experiment with

Figure 8. Continued

respect to unstimulated; symbols represent the value from each experiment; solid symbols indicating values of blot shown; bars indicate mean. Statistics represent mean \pm SEM. (C, F, I, L, O, and R) The *Skap2*^{-/-} values were divided by WT values in each respective experiment. The average WT level was set to 1 and is indicated by the dotted line. Data were compiled from n = 2–4 independent experiments. Significance was assessed using unpaired one-way ANOVA within each group, or two-way ANOVA between WT and KO groups with Sidak's post-test except for (E) which used paired two-way ANOVA with Sidak's post-test. See also [Tables S5–S9](#).

and furfuran-induced Pyk2 phosphorylation ([Figures 7G–7I](#) and [S4](#), [Tables S3](#) and [S4](#)). On the other hand, *C. glabrata* and *C. albicans*-induced Pyk2 phosphorylation was reduced in *Skap2*^{-/-} DIV neutrophils with the SKAP2-defect more pronounced in *C. glabrata*-stimulated conditions ([Figures 7J–7L](#) and [S4](#), [Tables S2](#) and [S4](#)). In summary, after infection with *C. glabrata* and *C. albicans*, Pyk2, but not Syk phosphorylation is reduced in the absence of SKAP2, whereas after infection with *K. pneumoniae*, the phosphorylation of both kinases requires SKAP2 ([Figures 7](#) and [S4](#)) ([Nguyen et al., 2020](#)).

Optimal *C. glabrata* and *K. pneumoniae*-induced phosphorylation of ERK1/2 and p38 requires SKAP2

In addition to tyrosine kinases, ROS production requires the activation and function of mitogen-activated protein kinases (MAPK) including extracellular signal regulated kinases (ERK)-1/2 and p38 ([Brown et al., 2004](#); [Dang et al., 2003, 2006](#); [Makni-Maalej et al., 2013](#)). Consistent with published data ([Makni-Maalej et al., 2013](#); [Li et al., 2011](#); [Lee et al., 2012](#); [Wozniok et al., 2008](#)), stimulation with TDB, furfuran, and *C. albicans* increased the phosphorylation of ERK1/2 and p38 10–200-fold higher than in unstimulated controls ([Figures 8A–8L](#), [Tables S5–S8](#)). To assess whether *C. glabrata* and *K. pneumoniae* lead to the phosphorylation of MAPKs, western blots of lysates from *C. glabrata* and *K. pneumoniae*-infected WT neutrophils were probed with phospho-specific antibodies. Infection with each pathogen induced significant phosphorylation of ERK1/2 and p38 relative to unstimulated controls ([Figures 8G–8R](#), [Tables S7–S10](#)). Because *Skap2*^{-/-} is required for maximal integrin-stimulated ERK1/2 phosphorylation ([Boras et al., 2017](#); [Shaban et al., 2020](#)), the phosphorylation of ERK1/2 and p38 following stimulation with TDB, furfuran, *C. albicans*, *C. glabrata*, and *K. pneumoniae* was assessed. While the stimulation of *Skap2*^{-/-} DIV neutrophils with all stimuli induced ERK phosphorylation, the fold induction triggered by TDB, *C. glabrata*, and *K. pneumoniae* was significantly lower than that seen in WT neutrophils ([Figures 8A–8C](#), [8G–8I](#), and [8M–8O](#)). Likewise, the phosphorylation of p38 was induced in *Skap2*^{-/-} neutrophils, however, the phosphorylation levels stimulated by *C. glabrata*, and *K. pneumoniae* were significantly lower than levels in WT ([Figures 8D–8F](#), [8J–8L](#), and [8P–8R](#)). As ERK1/2 and p38 can directly phosphorylate NADPH subunits ([Brown et al., 2004](#); [Dang et al., 2003, 2006](#)), the cumulative reduction of ERK1/2, and p38 activity in *Skap2*^{-/-} may contribute to the loss of ROS production downstream of *C. glabrata* ([Figure 5](#)), and *K. pneumoniae* ([Nguyen et al., 2020](#)).

DISCUSSION

Collectively, our results show that SKAP2 plays a critical role in optimal neutrophilic fungicidal responses to *C. glabrata* and to a lesser extent to *C. albicans*. In ROS induction, killing assays, and Western blot analyses of Pyk2, ERK1/2, and p38 phosphorylation, *C. glabrata* was consistently more dependent on SKAP2 than was *C. albicans* ([Figures 5](#), [6](#), [7](#), and [8](#)). These differences could be attributed to different morphologies and/or cell wall composition ([Brunke and Hube, 2013](#); [Dujon et al., 2004](#)). Prior work using human neutrophils showed that *C. albicans* and *C. glabrata* induce different levels of neutrophil activation, ROS, and phagocytosis ([Duggan et al., 2015](#)), potentially due to differences in the N-mannan structures, and the glucan exposure geometries at the molecular level ([Graus et al., 2018](#)). This is consistent with the idea that these pathogens do not trigger identical receptors on neutrophils and that signaling from some of these receptors is more dependent on SKAP2 than from others. Nonetheless, work using knockout mice showed that both Dectin-1 and Dectin-2 greatly contribute to the protection of mice against systemic *C. albicans* and *C. glabrata* infection ([Thompson et al., 2019](#); [Ifrim et al., 2014](#)). Thus, our observations that SKAP2 is important for ROS production and adhesion after stimulation by Dectin-1 and Dectin-2 ligands ([Figures 2](#), [3](#), and [5](#)) suggests that *Skap2*^{-/-} deficiencies may lead to attenuated responses against systemic *C. albicans* and *C. glabrata*. Additional studies in mouse lacking SKAP2 in neutrophils, in myeloid cells, or in all cells are required to establish the role of SKAP2 protection against *C. glabrata* and *C. albicans* infections in a mammalian host.

Prior work and our data here revealed that infection of neutrophils with *C. glabrata*, *C. albicans* or *K. pneumoniae* triggers signaling cascade(s) that require SFKs, Btk Syk, and SKAP2 pathway(s) leading

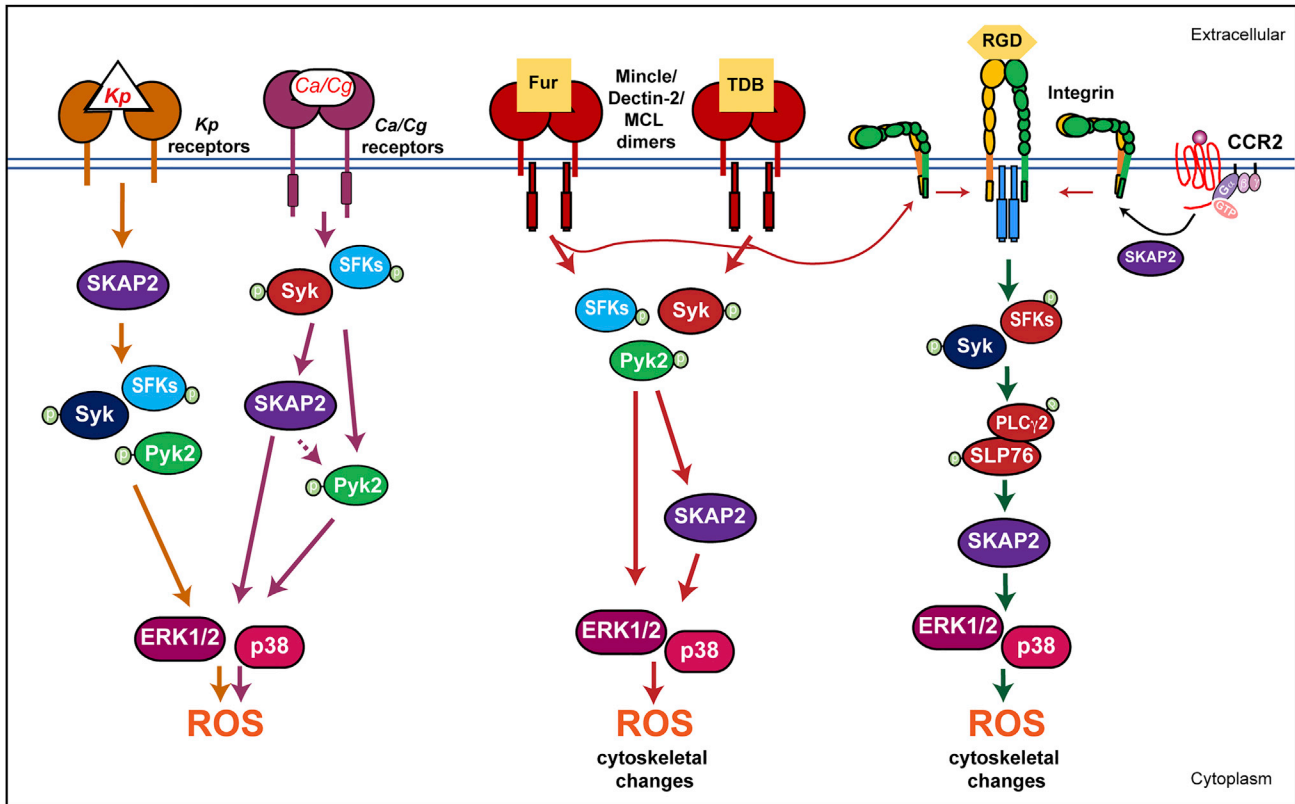


Figure 9. SKAP2 functions prior to or after Syk activation after infection with different pathogens

The binding of *K. pneumoniae* to surface receptors on neutrophils leads to the SKAP2-mediated phosphorylation of Syk and/or Pyk2 and requires the production of extracellular ROS. The binding of *C. glabrata* and *C. albicans* does not require SKAP2 for Syk phosphorylation; however, Pyk2 phosphorylation was dependent on SKAP2. Binding by the CLR agonist, furfuran and TBD induces Syk and Pyk phosphorylation independently of SKAP2. Likewise, SKAP2 contributes to extracellular ROS production and cell adhesion following the stimulation of integrins and fMLP (Nguyen et al., 2020; Boras et al., 2017; Shaban et al., 2020).

to ROS production (Figures 5 and 6) (Nguyen et al., 2020; Gazendam et al., 2014). However, after infection with these pathogens or stimulation with CLR agonist, we detected distinct differences in the requirements for SKAP2 for phosphorylation of Syk, Pyk2, ERK1/2, and p38 (Figures 7, 8, and S4 and (Nguyen et al., 2020)). Previous work had shown that Syk tyrosine phosphorylation is required signaling downstream of many receptors including CLR and integrin, while Pyk2 is required for integrin-mediated degranulation, but not ROS production (Kamen et al., 2011; Zarbock et al., 2007; Mocsai et al., 2002, 2003; Gazendam et al., 2014; Futosi et al., 2013). Since SKAP2 was not required for Syk phosphorylation after CLR, integrin, *C. albicans* or *C. glabrata* stimulation, but was required after *K. pneumoniae* stimulation (Figures 7A–7F and S4C, and (Shaban et al., 2020; Nguyen et al., 2020)), the receptor(s) that predominantly sense *K. pneumoniae* infection requires SKAP2 prior to Syk, Pyk2, ERK1/2, and p38 phosphorylation (Figure 9). These are distinct from those that recognize *C. glabrata* and *C. albicans*. Such receptors could include GPCRs, which have been shown to require SKAP2 for ROS and other functions, but are unlikely to be integrin or the CLR studied here (Boras et al., 2017; Sharma et al., 2014, 2017; Castillo et al., 2019; Shaban et al., 2020). By contrast, the receptors that recognize *C. glabrata* and *C. albicans* as well as CLR trigger activation Syk prior to, or potentially independently, of SKAP2 activation (Figure 7). Since SKAP2 was required for maximal phosphorylation of Pyk2, ERK1/2, and p38 after *C. glabrata* infection, but not after stimulation of Mincle or Dectin-2 (Figures 7 and 8), at least one other *C. glabrata* receptor requires SKAP2 for Pyk2, ERK1/2, and p38 phosphorylation and this potentially contributes to the stronger SKAP2-dependent fungicidal activities observed for *C. glabrata* (Figures 5D and 5E).

In summary, our findings broaden the spectrum of pattern recognition receptors that depend on SKAP2 for the activation of neutrophil ROS production and extend the role of SKAP2 in host defense beyond antibacterial

immunity to include *Candida* species. Mouse infection studies with *C. glabrata* are needed to further extend the importance of these findings to host defense against *C. glabrata* infection *in vivo*. Elucidating the mechanism(s) by which SKAP2 differently mediates signaling circuits leading to the activation of neutrophil ROS production after exposure to diverse pathogens is a focus of our future studies. There are differences between murine and human neutrophils that have been identified, including the expression of some receptors (Sun et al., 2016; Hajjar et al., 2010; Bagaitkar et al., 2012; Bengoechea and Sa Pessoa, 2019). However, the crucial function of SKAP2-mediated ROS in murine neutrophils following CLR, *C. albicans*, *C. glabrata*, and *K. pneumoniae* stimulation, and the findings that ROS requires Syk, SFK and Btk in both human and murine neutrophils suggests that parallels exist in signaling through CLR (Figures 6, 7, 8, and 9). Therefore, human neutrophils may also depend on SKAP2 for these responses. Further linkage studies showing association of Skap2 with autoimmune diseases (Barrett et al., 2009; Jostins et al., 2012), with over 600 *Skap2* variants/mutations reported in the human population across many age and ethnic groups (Karczewski et al., 2020), indicates that analysis of SKAP2 in human neutrophils and other cells is warranted.

Limitations of the study

A limitation to this study is that we have not infected *Skap2*^{-/-} mice with *C. glabrata*. These studies will be important to extend our findings leading to a more comprehensive understanding of host defense against *C. glabrata* infections *in vivo*. Growing evidence shows that neutrophils are dynamic cells that have different functional phenotypes during inflammation (Ng et al., 2019; Rosales, 2020). For example, neutrophils can undergo substantial changes in response to microenvironmental signals that appears to primarily be regulated by the microbiome and their ability to control infection can change with age of the individual (Zhang et al., 2015; Adrover et al., 2016). There are also differences between human and murine neutrophils. To enable the study of the signaling cascades regulating neutrophil activation and functions after infection with these microbes, murine neutrophils generated from HoxB8-immortalized murine progenitors were used in this study. In our experimental conditions, SKAP2 is required for the activation of ROS in response to C-type lectin stimulation and *C. albicans* and *C. glabrata* infections. The optimal phosphorylation of tyrosine kinase Pyk2, MAPK ERK1/2 and p38 following Mincle, *K. pneumoniae* and *C. glabrata* stimulation depends on SKAP2 functions. New studies are required to pinpoint the structure-function relationship between SKAP2 and other components in these signal transduction pathways, and then to extend these findings in neutrophils from mice to humans.

STAR★METHODS

Detailed methods are provided in the online version of this paper and include the following:

- KEY RESOURCES TABLE
- RESOURCE AVAILABILITY
 - Lead contact
 - Materials availability
 - Data and code availability
- EXPERIMENTAL MODEL AND SUBJECT DETAILS
 - Animals
 - Bone marrow neutrophil isolation
 - HoxB8 cell culture system
 - Human neutrophil isolation
 - Bacterial and fungal strains
- METHOD DETAILS
 - Flow cytometry
 - DIV neutrophil *in vivo* transfer experiment
 - C-type lectin receptors (CLRs) expression
 - Neutrophil ROS assays
 - Spreading/adhesion assay
 - Integrin activation
 - Neutrophil killing of *Candida*
 - Western blot analysis
- QUANTIFICATION AND STATISTICAL ANALYSIS

SUPPLEMENTAL INFORMATION

Supplemental information can be found online at <https://doi.org/10.1016/j.isci.2021.102871>.

ACKNOWLEDGMENTS

We thank Lamyaa Shaban, Alyssa Fasciano, Rebecca Silver, Anne McCabe, Michelle Sodipo, Parisa Kalantari, Miles Duncan, Maria-Cristina Seminario and Kenneth Swanson for critically reading the manuscript and/or for helpful scientific and technical discussions. This work was supported by NIH NIAID R01 AI113166 award to JM, NIH NIAID R21 AG071268 awarded to JM and JML, and NIH NIAID RO1 AI132638 to MKM, and NIH K12GM074869 supported W.A (Dr. Claire Moore, PI). The authors declare no competing financial interests.

AUTHOR CONTRIBUTIONS

Conceptualization, G.T.N., S.C.B., J.M.; data curation, G.T.N., S.X., J.M.; formal analysis, G.T.N., S.X., J.M.; funding acquisition, J.M., M.M. J.M.L.; investigation, G.T.N., S.X., W.A., D.B.S.; methodology, G.T.N., S.X., W.A. D.B.S.; resources, J.M.L., S.C.B., M.M., D.B.S., J.M.; supervision J.M.L., M.M., J.M.; visualization, G.T.N.; writing – original draft preparation, G.T.N.; writing – review & editing, G.T.N., S.X., W.A., J.M.L., S.C.B., M.M., D.B.S., J.M.; project administration, J.M.

DECLARATION OF INTERESTS

The authors declare no competing interests.

Received: April 19, 2021

Revised: June 3, 2021

Accepted: July 14, 2021

Published: August 20, 2021

REFERENCES

- Adams, W., Bhowmick, R., Bou Ghanem, E.N., Wade, K., Shchepetov, M., Weiser, J.N., McCormick, B.A., Tweten, R.K., and Leong, J.M. (2020). Pneumolysin induces 12-lipoxygenase-dependent neutrophil migration during *Streptococcus pneumoniae* infection. *J. Immunol.* *204*, 101–111.
- Adams, W., Espicha, T., and Estipona, J. (2021). Getting your neutrophil: neutrophil transepithelial migration in the lung. *Infect. Immun.* <https://doi.org/10.1128/IAI.00659-20>.
- Adrover, J.M., Nicolas-Avila, J.A., and Hidalgo, A. (2016). Aging: a temporal dimension for neutrophils. *Trends Immunol.* *37*, 334–345.
- Alenghat, F.J., Baca, Q.J., Rubin, N.T., Pao, L.I., Matozaki, T., Lowell, C.A., Golan, D.E., Neel, B.G., and Swanson, K.D. (2012). Macrophages require Skap2 and Sirpalpha for integrin-stimulated cytoskeletal rearrangement. *J. Cell Sci.* *125*, 5535–5545.
- Arendrup, M.C., Bruun, B., Christensen, J.J., Fuursted, K., Johansen, H.K., Kjaeldgaard, P., Knudsen, J.D., Kristensen, L., Moller, J., Nielsen, L., et al. (2011). National surveillance of fungemia in Denmark (2004 to 2009). *J. Clin. Microbiol.* *49*, 325–334.
- Bagaitkar, J., Matute, J.D., Austin, A., Arias, A.A., and Dinauer, M.C. (2012). Activation of neutrophil respiratory burst by fungal particles requires phosphatidylinositol 3-phosphate binding to p40(phox) in humans but not in mice. *Blood* *120*, 3385–3387.
- Barrett, J.C., Clayton, D.G., Concannon, P., Akolkar, B., Cooper, J.D., Erlich, H.A., Julier, C., Morahan, G., Nerup, J., Nierras, C., et al. (2009). Genome-wide association study and meta-analysis find that over 40 loci affect risk of type 1 diabetes. *Nat. Genet.* *41*, 703–707.
- Bengoechea, J.A., and Sa Pessoa, J. (2019). *Klebsiella pneumoniae* infection biology: living to counteract host defences. *FEMS Microbiol. Rev.* *43*, 123–144.
- Boras, M., Volmering, S., Bokemeyer, A., Rossaint, J., Block, H., Bardel, B., Van Marck, V., Heitplatz, B., Kliche, S., Reinhold, A., et al. (2017). Skap2 is required for beta2 integrin-mediated neutrophil recruitment and functions. *J. Exp. Med.* *214*, 851–874.
- Bortoletto, P., Lyman, K., Camacho, A., Fricchione, M., Khanolkar, A., and Katz, B.Z. (2015). Chronic granulomatous disease: a large, single-center US experience. *Pediatr. Infect. Dis. J.* *34*, 1110–1114.
- Brown, G.D., Herre, J., Williams, D.L., Willment, J.A., Marshall, A.S., and Gordon, S. (2003). Dectin-1 mediates the biological effects of beta-glucans. *J. Exp. Med.* *197*, 1119–1124.
- Brown, G.E., Stewart, M.Q., Bissonnette, S.A., Elia, A.E., Wilker, E., and Yaffe, M.B. (2004). Distinct ligand-dependent roles for p38 MAPK in priming and activation of the neutrophil NADPH oxidase. *J. Biol. Chem.* *279*, 27059–27068.
- Brunke, S., and Hube, B. (2013). Two unlike cousins: *Candida albicans* and *C. glabrata* infection strategies. *Cell. Microbiol.* *15*, 701–708.
- Castillo, L.A., Birnberg-Weiss, F., Rodriguez-Rodriguez, N., Martire-Greco, D., Bigi, F., Landoni, V.I., Gomez, S.A., and Fernandez, G.C. (2019). *Klebsiella pneumoniae* ST258 negatively regulates the oxidative burst in human neutrophils. *Front. Immunol.* *10*, 929.
- Chen, S.M., Shen, H., Zhang, T., Huang, X., Liu, X.Q., Guo, S.Y., Zhao, J.J., Wang, C.F., Yan, L., Xu, G.T., et al. (2017). Dectin-1 plays an important role in host defense against systemic *Candida glabrata* infection. *Virulence* *8*, 1643–1656.
- Chu, J.Y., McCormick, B., Mazelyte, G., Michael, M., and Vermeren, S. (2019). HoxB8 neutrophils replicate Fcgamma receptor and integrin-induced neutrophil signaling and functions. *J. Leukoc. Biol.* *105*, 93–100.
- Colado, A., Marin Franco, J.L., Elias, E.E., Amondarain, M., Vergara Rubio, M., Sarapura Martinez, V., Cordini, G., Fuentes, F., Balboa, L., Fernandez Grecco, H., et al. (2020). Second generation BTK inhibitors impair the anti-fungal response of macrophages and neutrophils. *Am. J. Hematol.* *95*, E174–E178.
- Dahlgren, C., Bjornsdottir, H., Sundqvist, M., Christenson, K., and Bylund, J. (2020). Measurement of respiratory burst products, released or retained, during activation of professional phagocytes. *Methods Mol. Biol.* *2087*, 301–324.

- Dambuzza, I.M., and Brown, G.D. (2015). C-type lectins in immunity: recent developments. *Curr. Opin. Immunol.* 32, 21–27.
- Dang, P., Stensballe, A., Boussetta, T., Raad, H., Dewas, C., Kroviarski, Y., Hayem, G., Jensen, O.N., Gougerot-Pocidal, M.A., and El-Benna, J. (2006). A specific p47phox-serine phosphorylated by convergent MAPKs mediates neutrophil NADPH oxidase priming at inflammatory sites. *J. Clin. Invest.* 116, 2033–2043.
- Dang, P.M., Morel, F., Gougerot-Pocidal, M.A., and El Benna, J. (2003). Phosphorylation of the NADPH oxidase component p67(PHOX) by ERK2 and P38MAPK: selectivity of phosphorylated sites and existence of an intramolecular regulatory domain in the tetratricopeptide-rich region. *Biochemistry* 42, 4520–4526.
- Deng, Z., Ma, S., Zhou, H., Zang, A., Fang, Y., Li, T., Shi, H., Liu, M., Du, M., Taylor, P.R., et al. (2015). Tyrosine phosphatase SHP-2 mediates C-type lectin receptor-induced activation of the kinase Syk and anti-fungal TH17 responses. *Nat. Immunol.* 16, 642–652.
- Dransfield, I., Cabanas, C., Craig, A., and Hogg, N. (1992). Divalent cation regulation of the function of the leukocyte integrin LFA-1. *J. Cell Biol.* 116, 219–226.
- Duggan, S., Essig, F., Hunniger, K., Mokhtari, Z., Bauer, L., Lehnert, T., Brandes, S., Hader, A., Jacobsen, I.D., Martin, R., et al. (2015). Neutrophil activation by *Candida glabrata* but not *Candida albicans* promotes fungal uptake by monocytes. *Cell. Microbiol.* 17, 1259–1276.
- Dujon, B., Sherman, D., Fischer, G., Durrens, P., Casaregola, S., Lafontaine, I., De Montigny, J., Marck, C., Neuvéglise, C., Talla, E., et al. (2004). Genome evolution in yeasts. *Nature* 430, 35–44.
- El Benna, J., Ruedi, J.M., and Babior, B.M. (1994). Cytosolic guanine nucleotide-binding protein Rac2 operates in vivo as a component of the neutrophil respiratory burst oxidase. Transfer of Rac2 and the cytosolic oxidase components p47phox and p67phox to the submembranous actin cytoskeleton during oxidase activation. *J. Biol. Chem.* 269, 6729–6734.
- Fagerholm, S.C., Guenther, C., Lloret Asens, M., Savinko, T., and Uotila, L.M. (2019). Beta2-Integrins and interacting proteins in leukocyte trafficking, immune suppression, and immunodeficiency disease. *Front. Immunol.* 10, 254.
- Feinberg, H., Jegouzo, S.A.F., Rex, M.J., Drickamer, K., Weis, W.I., and Taylor, M.E. (2017). Mechanism of pathogen recognition by human dectin-2. *J. Biol. Chem.* 292, 13402–13414.
- Ferwerda, B., Ferwerda, G., Plantinga, T.S., Willment, J.A., Van Spruiel, A.B., Venselaar, H., Elbers, C.C., Johnson, M.D., Cambi, A., Huysamen, C., et al. (2009). Human dectin-1 deficiency and mucocutaneous fungal infections. *N. Engl. J. Med.* 361, 1760–1767.
- Futosi, K., Fodor, S., and Mocsai, A. (2013). Neutrophil cell surface receptors and their intracellular signal transduction pathways. *Int. Immunopharmacol.* 17, 638–650.
- Gazendam, R.P., Van Hamme, J.L., Tool, A.T., Van Houdt, M., Verkuiljen, P.J., Herbst, M., Liese, J.G., Van De Veerndonk, F.L., Roos, D., Van Den Berg, T.K., and Kuijpers, T.W. (2014). Two Independent killing mechanisms of *Candida albicans* by human neutrophils: evidence from innate immunity defects. *Blood* 124, 590–597.
- Graus, M.S., Wester, M.J., Lowman, D.W., Williams, D.L., Kruppa, M.D., Martinez, C.M., Young, J.M., Pappas, H.C., Lidke, K.A., and Neumann, A.K. (2018). Mannan molecular substructures control nanoscale glucan exposure in *Candida*. *Cell Rep.* 24, 2432–2442 e5.
- Hajjar, E., Broemstrup, T., Kantari, C., Witko-Sarsat, V., and Reuter, N. (2010). Structures of human proteinase 3 and neutrophil elastase—so similar yet so different. *FEBS J.* 277, 2238–2254.
- Hopke, A., Scherer, A., Kreuzburg, S., Abers, M.S., Zerbe, C.S., Dinauer, M.C., Mansour, M.K., and Irimia, D. (2020). Neutrophil swarming delays the growth of clusters of pathogenic fungi. *Nat. Commun.* 11, 2031.
- Ifrim, D.C., Bain, J.M., Reid, D.M., Oosting, M., Verschuere, I., Gow, N.A., Van Krieken, J.H., Brown, G.D., Kullberg, B.J., Joosten, L.A., et al. (2014). Role of Dectin-2 for host defense against systemic infection with *Candida glabrata*. *Infect. Immun.* 82, 1064–1073.
- Jakus, Z., Nemeth, T., Verbeek, J.S., and Mocsai, A. (2008). Critical but overlapping role of FcγRIII and FcγRIV in activation of murine neutrophils by immobilized immune complexes. *J. Immunol.* 180, 618–629.
- Jostins, L., Ripke, S., Weersma, R.K., Duerr, R.H., McGovern, D.P., Hui, K.Y., Lee, J.C., Schumm, L.P., Sharma, Y., Anderson, C.A., et al. (2012). Host-microbe interactions have shaped the genetic architecture of inflammatory bowel disease. *Nature* 491, 119–124.
- Kamen, L.A., Schlessinger, J., and Lowell, C.A. (2011). Pyk2 is required for neutrophil degranulation and host defense responses to bacterial infection. *J. Immunol.* 186, 1656–1665.
- Karczewski, K.J., Francioli, L.C., Tiao, G., Cummings, B.B., Alföldi, J., Wang, Q., Collins, R.L., Laricchia, K.M., Ganna, A., Birnbaum, D.P., et al. (2020). The mutational constraint spectrum quantified from variation in 141,456 humans. *Nature* 581, 434–443.
- Kobayashi, S.D., Porter, A.R., Dorward, D.W., Brinkworth, A.J., Chen, L., Kreiswirth, B.N., and Deleo, F.R. (2016). Phagocytosis and killing of carbapenem-resistant ST258 *Klebsiella pneumoniae* by human neutrophils. *J. Infect. Dis.* 213, 1615–1622.
- Lee, W.B., Kang, J.S., Yan, J.J., Lee, M.S., Jeon, B.Y., Cho, S.N., and Kim, Y.J. (2012). Neutrophils promote mycobacterial trehalose dimycolate-induced lung inflammation via the mincle pathway. *PLoS Pathog.* 8, e1002614.
- Lee, W.B., Yan, J.J., Kang, J.S., Zhang, Q., Choi, W.Y., Kim, L.K., and Kim, Y.J. (2017). Mincle activation enhances neutrophil migration and resistance to polymicrobial septic peritonitis. *Sci. Rep.* 7, 41106.
- Li, X., Utomo, A., Cullere, X., Choi, M.M., Milner, D.A., Jr., Venkatesh, D., Yun, S.H., and Mayadas, T.N. (2011). The beta-glucan receptor Dectin-1 activates the integrin Mac-1 in neutrophils via Vav protein signaling to promote *Candida albicans* clearance. *Cell Host Microbe* 10, 603–615.
- Makni-Maalej, K., Chiantotto, M., Hurtado-Nedelec, M., Bedouhene, S., Gougerot-Pocidal, M.A., Dang, P.M., and El-Benna, J. (2013). Zymosan induces NADPH oxidase activation in human neutrophils by inducing the phosphorylation of p47phox and the activation of Rac2: involvement of protein tyrosine kinases, PI3Kinase, PKC, ERK1/2 and p38MAPKinase. *Biochem. Pharmacol.* 85, 92–100.
- Mansour, M.K., Tam, J.M., Khan, N.S., Seward, M., Davids, P.J., Puranam, S., Sokolovska, A., Sykes, D.B., Dagher, Z., Becker, C., et al. (2013). Dectin-1 activation controls maturation of beta-1,3-glucan-containing phagosomes. *J. Biol. Chem.* 288, 16043–16054.
- McGreal, E.P., Rosas, M., Brown, G.D., Zamze, S., Wong, S.Y., Gordon, S., Martinez-Pomares, L., and Taylor, P.R. (2006). The carbohydrate-recognition domain of Dectin-2 is a C-type lectin with specificity for high mannose. *Glycobiology* 16, 422–430.
- Mocsai, A., Zhang, H., Jakus, Z., Kitauro, J., Kawakami, T., and Lowell, C.A. (2003). G-protein-coupled receptor signaling in Syk-deficient neutrophils and mast cells. *Blood* 101, 4155–4163.
- Mocsai, A., Zhou, M., Meng, F., Tybulewicz, V.L., and Lowell, C.A. (2002). Syk is required for integrin signaling in neutrophils. *Immunity* 16, 547–558.
- Nani, S., Fumagalli, L., Sinha, U., Kamen, L., Scapini, P., and Berton, G. (2015). Src family kinases and Syk are required for neutrophil extracellular trap formation in response to beta-glucan particles. *J. Innate Immun.* 7, 59–73.
- Nauseef, W.M., Volpp, B.D., McCormick, S., Leidal, K.G., and Clark, R.A. (1991). Assembly of the neutrophil respiratory burst oxidase. Protein kinase C promotes cytoskeletal and membrane association of cytosolic oxidase components. *J. Biol. Chem.* 266, 5911–5917.
- Negoro, P.E., Xu, S., Dagher, Z., Hopke, A., Reedy, J.L., Feldman, M.B., Khan, N.S., Viens, A.L., Alexander, N.J., Atallah, N.J., et al. (2020). Spleen tyrosine kinase is a critical regulator of neutrophil responses to *Candida* species. *mBio* 11, e02043-19.
- Netea, M.G., Joosten, L.A., Van Der Meer, J.W., Kullberg, B.J., and Van De Veerndonk, F.L. (2015). Immune defence against *Candida* fungal infections. *Nat. Rev. Immunol.* 15, 630–642.
- Ng, L.G., Ostuni, R., and Hidalgo, A. (2019). Heterogeneity of neutrophils. *Nat. Rev. Immunol.* 19, 255–265.
- Nguyen, G.T., Green, E.R., and Mecsas, J. (2017). Neutrophils to the ROScUE: mechanisms of NADPH oxidase activation and bacterial resistance. *Front. Cell Infect. Microbiol.* 7, 373.
- Nguyen, G.T., Shaban, L., Mack, M., Swanson, K.D., Bunnell, S.C., Sykes, D.B., and Mecsas, J. (2020). SKAP2 is required for defense against *K. pneumoniae* infection and neutrophil respiratory burst. *Elife* 9, e56656.
- Ostrop, J., Jozefowski, K., Zimmermann, S., Hofmann, K., Strasser, E., Lepenies, B., and Lang, A. (2019). The beta-glucan receptor Dectin-1 activates the integrin Mac-1 in neutrophils via Vav protein signaling to promote *Candida albicans* clearance. *Cell Host Microbe* 10, 603–615.

- R. (2015). Contribution of MINCLE-SYK signaling to activation of primary human APCs by mycobacterial cord factor and the novel adjuvant TDB. *J. Immunol.* 195, 2417–2428.
- Ostrop, J., and Lang, R. (2017). Contact, collaboration, and conflict: signal integration of syk-coupled C-type lectin receptors. *J. Immunol.* 198, 1403–1414.
- Paczosa, M.K., Silver, R.J., McCabe, A.L., Tai, A.K., Mcleish, C.H., Lazinski, D.W., and Mecsas, J. (2020). Transposon mutagenesis screen of *Klebsiella pneumoniae* identifies multiple genes important for resisting antimicrobial activities of neutrophils in mice. *Infect. Immun.* 88, e00034–20.
- Pelletier, M.G., Szymczak, K., Barbeau, A.M., Prata, G.N., O'fallon, K.S., and Gaines, P. (2017). Characterization of neutrophils and macrophages from ex vivo-cultured murine bone marrow for morphologic maturation and functional responses by imaging flow cytometry. *Methods* 112, 124–146.
- Prevention, C.F.D.C.A. (2019). Antibiotic resistance threats in the United States, 2019. In: Centers for Disease Control and Prevention (U.S. Department of Health and Human Services).
- Rogers, N.C., Slack, E.C., Edwards, A.D., Nolte, M.A., Schulz, O., Schweighoffer, E., Williams, D.L., Gordon, S., Tybulewicz, V.L., Brown, G.D., and Reis E Sousa, C. (2005). Syk-dependent cytokine induction by Dectin-1 reveals a novel pattern recognition pathway for C type lectins. *Immunity* 22, 507–517.
- Rolan, H.G., Durand, E.A., and Mecsas, J. (2013). Identifying *Yersinia* YopH-targeted signal transduction pathways that impair neutrophil responses during in vivo murine infection. *Cell Host Microbe* 14, 306–317.
- Rosales, C. (2020). Neutrophils at the crossroads of innate and adaptive immunity. *J. Leukoc. Biol.* 108, 377–396.
- Saijo, S., Ikeda, S., Yamabe, K., Kakuta, S., Ishigame, H., Akitsu, A., Fujikado, N., Kusaka, T., Kubo, S., Chung, S.H., et al. (2010). Dectin-2 recognition of alpha-mannans and induction of Th17 cell differentiation is essential for host defense against *Candida albicans*. *Immunity* 32, 681–691.
- Sato, K., Yang, X.L., Yudate, T., Chung, J.S., Wu, J., Luby-Phelps, K., Kimberly, R.P., Underhill, D., Cruz, P.D., Jr., and Ariizumi, K. (2006). Dectin-2 is a pattern recognition receptor for fungi that couples with the Fc receptor gamma chain to induce innate immune responses. *J. Biol. Chem.* 281, 38854–38866.
- Saul, S., Castelbou, C., Fickentscher, C., and Demaurex, N. (2019). Signaling and functional competency of neutrophils derived from bone-marrow cells expressing the ER-HOXB8 oncoprotein. *J. Leukoc. Biol.* 106, 1101–1115.
- Shaban, L., Nguyen, G.T., Mecsas-Faxon, B.D., Swanson, K.D., Tan, S., and Mecsas, J. (2020). *Yersinia pseudotuberculosis* YopH targets SKAP2-dependent and independent signaling pathways to block neutrophil antimicrobial mechanisms during infection. *PLoS Pathog.* 16, e1008576.
- Sharma, A., Simonson, T.J., Jondle, C.N., Mishra, B.B., and Sharma, J. (2017). Mincle-mediated neutrophil extracellular trap formation by regulation of autophagy. *J. Infect. Dis.* 215, 1040–1048.
- Sharma, A., Steichen, A.L., Jondle, C.N., Mishra, B.B., and Sharma, J. (2014). Protective role of Mincle in bacterial pneumonia by regulation of neutrophil mediated phagocytosis and extracellular trap formation. *J. Infect. Dis.* 209, 1837–1846.
- Silva, S., Negri, M., Henriques, M., Oliveira, R., Williams, D.W., and Azeredo, J. (2012). *Candida glabrata*, *Candida parapsilosis* and *Candida tropicalis*: biology, epidemiology, pathogenicity and antifungal resistance. *FEMS Microbiol. Rev.* 36, 288–305.
- Silver, R.J., Paczosa, M.K., McCabe, A.L., Balada-Llasat, J.M., Baleja, J.D., and Mecsas, J. (2019). Amino acid Biosynthetic pathways are required for *Klebsiella pneumoniae* growth in immunocompromised lungs and are druggable targets during infection. *Antimicrob. Agents Chemother.* 63, e02674–18.
- Strasser, D., Neumann, K., Bergmann, H., Marakalala, M.J., Guler, R., Rojowska, A., Hopfner, K.P., Brombacher, F., Urlaub, H., Baier, G., et al. (2012). Syk kinase-coupled C-type lectin receptors engage protein kinase C-sigma to elicit Card9 adaptor-mediated innate immunity. *Immunity* 36, 32–42.
- Strijbis, K., Tafesse, F.G., Fair, G.D., Witte, M.D., Dougan, S.K., Watson, N., Spooner, E., Esteban, A., Vyas, V.K., Fink, G.R., et al. (2013). Bruton's Tyrosine Kinase (BTK) and Vav1 contribute to Dectin1-dependent phagocytosis of *Candida albicans* in macrophages. *PLoS Pathog.* 9, e1003446.
- Sun, J., Li, N., Oh, K.S., Dutta, B., Vaytaden, S.J., Lin, B., Ebert, T.S., De Nardo, D., Davis, J., Bagirzadeh, R., et al. (2016). Comprehensive RNAi-based screening of human and mouse TLR pathways identifies species-specific preferences in signaling protein use. *Sci. Signal.* 9, ra3.
- Sykes, D.B., and Kamps, M.P. (2001). Estrogen-dependent E2a/Pbx1 myeloid cell lines exhibit conditional differentiation that can be arrested by other leukemic oncoproteins. *Blood* 98, 2308–2318.
- Tam, J.M., Reedy, J.L., Lukason, D.P., Kuna, S.G., Acharya, M., Khan, N.S., Negoro, P.E., Xu, S., Ward, R.A., Feldman, M.B., et al. (2019). Tetraspanin CD82 organizes dectin-1 into signaling domains to mediate cellular responses to *Candida albicans*. *J. Immunol.* 202, 3256–3266.
- Tanaka, M., Shimamura, S., Kuriyama, S., Maeda, D., Goto, A., and Aiba, N. (2016). SKAP2 promotes podosome formation to facilitate tumor-associated macrophage infiltration and metastatic progression. *Cancer Res.* 76, 358–369.
- Taylor, P.R., Tsoni, S.V., Willment, J.A., Dennehy, K.M., Rosas, M., Findon, H., Haynes, K., Steele, C., Botto, M., Gordon, S., and Brown, G.D. (2007). Dectin-1 is required for beta-glucan recognition and control of fungal infection. *Nat. Immunol.* 8, 31–38.
- Thompson, A., Davies, L.C., Liao, C.T., Da Fonseca, D.M., Griffiths, J.S., Andrews, R., Jones, A.V., Clement, M., Brown, G.D., Humphreys, I.R., et al. (2019). The protective effect of inflammatory monocytes during systemic *C. albicans* infection is dependent on collaboration between C-type lectin-like receptors. *PLoS Pathog.* 15, e1007850.
- Togni, M., Swanson, K.D., Reimann, S., Kliche, S., Pearce, A.C., Simeoni, L., Reinhold, D., Wienands, J., Neel, B.G., Schraven, B., and Gerber, A. (2005). Regulation of in vitro and in vivo immune functions by the cytosolic adaptor protein SKAP-HOM. *Mol. Cell. Biol.* 25, 8052–8063.
- Tortorano, A.M., Kibbler, C., Peman, J., Bernhardt, H., Klingspor, L., and Grillot, R. (2006). *Candidaemia* in Europe: epidemiology and resistance. *Int. J. Antimicrob. Agents* 27, 359–366.
- Van Strijp, J.A., Russell, D.G., Tuomanen, E., Brown, E.J., and Wright, S.D. (1993). Ligand specificity of purified complement receptor type three (CD11b/CD18, alpha m beta 2, Mac-1). Indirect effects of an Arg-Gly-Asp (RGD) sequence. *J. Immunol.* 151, 3324–3336.
- Wang, G.G., Calvo, K.R., Pasillas, M.P., Sykes, D.B., Hacker, H., and Kamps, M.P. (2006). Quantitative production of macrophages or neutrophils ex vivo using conditional Hoxb8. *Nat. Methods* 3, 287–293.
- Wells, C.A., Salvage-Jones, J.A., Li, X., Hitchens, K., Butcher, S., Murray, R.Z., Beckhouse, A.G., Lo, Y.L., Manzanero, S., Cobbold, C., et al. (2008). The macrophage-inducible C-type lectin, mincle, is an essential component of the innate immune response to *Candida albicans*. *J. Immunol.* 180, 7404–7413.
- Wolach, B., Gavrieli, R., De Boer, M., Van Leeuwen, K., Berger-Achituv, S., Stauber, T., Ben Ari, J., Rottem, M., Schlesinger, Y., Grisaru-Soen, G., et al. (2017). Chronic granulomatous disease: clinical, functional, molecular, and genetic studies. The Israeli experience with 84 patients. *Am. J. Hematol.* 92, 28–36.
- Woodman, R.C., Ruedi, J.M., Jesaitis, A.J., Okamura, N., Quinn, M.T., Smith, R.M., Curnutte, J.T., and Babior, B.M. (1991). Respiratory burst oxidase and three of four oxidase-related polypeptides are associated with the cytoskeleton of human neutrophils. *J. Clin. Invest.* 87, 1345–1351.
- Wozniok, I., Hornbach, A., Schmitt, C., Frosch, M., Einsele, H., Hube, B., Löffler, J., and Kurzai, O. (2008). Induction of Erk-Kinase signalling triggers morphotype-specific killing of *Candida albicans* filaments by human neutrophils. *Cell Microbiol.* 10, 807–820.
- Wu, S.Y., Weng, C.L., Jheng, M.J., Kan, H.W., Hsieh, S.T., Liu, F.T., and Wu-Hsieh, B.A. (2019). *Candida albicans* triggers NADPH oxidase-independent neutrophil extracellular traps through dectin-2. *PLoS Pathog.* 15, e1008096.
- Xiong, H., Carter, R.A., Leiner, I.M., Tang, Y.W., Chen, L., Kreiswirth, B.N., and Pamer, E.G. (2015). Distinct contributions of neutrophils and CCR2+

monocytes to pulmonary clearance of different *Klebsiella pneumoniae* strains. *Infect. Immun.* 83, 3418–3427.

Xu, S., Feliu, M., Lord, A.K., Lukason, D.P., Negoro, P.E., Khan, N.S., Dagher, Z., Feldman, M.B., Reedy, J.L., Steiger, S.N., et al. (2018). Biguanides enhance antifungal activity against *Candida glabrata*. *Virulence* 9, 1150–1162.

Yamasaki, S., Ishikawa, E., Sakuma, M., Hara, H., Ogata, K., and Saito, T. (2008). Mincle is an ITAM-coupled activating receptor that senses damaged cells. *Nat. Immunol.* 9, 1179–1188.

Ye, F., Kim, C., and Ginsberg, M.H. (2012). Reconstruction of integrin activation. *Blood* 119, 26–33.

Ye, P., Rodriguez, F.H., Kanaly, S., Stocking, K.L., Schurr, J., Schwarzenberger, P., Oliver, P., Huang, W., Zhang, P., Zhang, J., et al. (2001). Requirement of interleukin 17 receptor signaling for lung CXC chemokine and granulocyte colony-stimulating factor expression, neutrophil recruitment, and host defense. *J. Exp. Med.* 194, 519–527.

Zarbock, A., Lowell, C.A., and Ley, K. (2007). Spleen tyrosine kinase Syk is necessary for E-selectin-induced $\alpha(L)\beta(2)$ integrin-

mediated rolling on intercellular adhesion molecule-1. *Immunity* 26, 773–783.

Zhang, D., Chen, G., Manwani, D., Mortha, A., Xu, C., Faith, J.J., Burk, R.D., Kunisaki, Y., Jang, J.E., Scheiermann, C., et al. (2015). Neutrophil ageing is regulated by the microbiome. *Nature* 525, 528–532.

Zhu, L.L., Zhao, X.Q., Jiang, C., You, Y., Chen, X.P., Jiang, Y.Y., Jia, X.M., and Lin, X. (2013). C-type lectin receptors Dectin-3 and Dectin-2 form a heterodimeric pattern-recognition receptor for host defense against fungal infection. *Immunity* 39, 324–334.

STAR★METHODS

KEY RESOURCES TABLE

REAGENT or RESOURCE	SOURCE	IDENTIFIER
Antibodies		
Rat Anti-Ly6G monoclonal antibody, unconjugated, Clone 1A8	Fisher Scientific	BD Biosciences Cat# 551459, RRID:AB_394206
Rat anti-mouse CD16/CD32 Mouse BD Fc Block	BD Biosciences	BD Biosciences Cat# 553142, RRID:AB_394657
Rat monoclonal anti-mouse/human a-CD11b-PE or a-CD11b-PacBlue(clone M1/70)	Biolegend	BioLegend Cat# 101207, RRID:AB_312790 BioLegend Cat# 101223, RRID:AB_755985
Rat monoclonal anti-mouse a-Ly6G PE-Cy7(clone 1A8)	Biolegend	BioLegend Cat# 127617, RRID:AB_1877262
Rat monoclonal anti-mouse a-Gr1-APC (clone RB6-8C5)	Biolegend	BioLegend Cat# 108405, RRID:AB_313370
Rat monoclonal anti-mouse a-Ly6C-AlexaFluor647(clone HK1.4)	BioLegend	BioLegend Cat# 128010, RRID:AB_1236550
Rabbit polyclonal anti-mouse/human a-SKAP2	Proteintech	Proteintech Cat# 12926-1-AP, RRID:AB_2189317
rabbit IgG polyclonal isotype antibody	Proteintech	Proteintech Cat# 30000-0-AP, RRID:AB_2819035
Alexa Fluor 488 goat anti-rabbit secondary antibody	Thermo Fisher Scientific	Thermo Fisher Scientific Cat# A-11034, RRID:AB_2576217
Rabbit polyclonal anti-human serum albumin	Sigma-Aldrich	Sigma-Aldrich Cat# A0433, RRID:AB_257887
Rabbit anti-human/mouse monoclonal Phospho-Zap-70 (Y319)/Syk (Y352)	Cell Signaling Technology	Cell Signaling Technology Cat# 2717, RRID:AB_2218658
Rabbit anti-human/mouse polyclonal Phospho-Pyk2 (Y402)	Cell Signaling Technology	Cell Signaling Technology Cat# 3291, RRID:AB_2300530
Rabbit anti-human/mouse polyclonal RhoGDI	Cell Signaling Technology	Cell Signaling Technology Cat# 2564, RRID:AB_2274313
Rabbit anti-human/mouse polyclonal Syk	Cell Signaling Technology	Cell Signaling Technology Cat# 2712, RRID:AB_2197223
Rabbit anti-human/mouse polyclonal Pyk2	Cell Signaling Technology	Cell Signaling Technology Cat# 3292, RRID:AB_2174097
Goat Anti-rabbit IgG (H+L) (DyLight™ 800 4X PEG Conjugate)	Cell Signaling Technology	Cell Signaling Technology Cat# 5151, RRID:AB_10697505
Rat anti-mouse Dectin-1	Biolegend	BioLegend Cat# 144302, RRID:AB_2561519
Rabbit anti-mouse Mincle	MyBioSource	Cat # MBS1497212 NCBI Accession # NP_055173.1
Biotinylated goat-anti-mouse Dectin-2	R&D Systems	BAF1525
APC-conjugated streptavidin antibodies	Biolegend	Cat# 405207
Alexa 594-conjugated goat anti-rat	Invitrogen	Catalog # A-11007 RRID AB_10561522
Alexa 594-labeled goat anti-rabbit	Invitrogen	Catalog # A-11012 RRID AB_2534079
ERK1/2-Thr202/Tyr204	Cell Signaling Technology	Cat #9102S UniProt ID: P27361, P28482
pp38-Thr180/Y182	Cell Signaling Technology	Cat #4511S UniProt ID: Q16539, O15264, P53778, Q15759

(Continued on next page)

Continued

REAGENT or RESOURCE	SOURCE	IDENTIFIER
ERK1/2	Cell Signaling Technology	Cat #4695S UniProt ID: P27361, P28482
p38	Cell Signaling Technology	Cat #8690S UniProt ID: Q16539, P53778, Q15759

Bacterial and virus strains

<i>Klebsiella pneumoniae</i> , ATCC 43816 KPPR1	GenBank ATCC	GenBank: CP009208.1
<i>C. albicans</i> (SC5314)	Michael Mansour	CandidaDB, RRID:SCR_007579
<i>C. glabrata</i> (ATCC, 2001)	Michael Mansour	Proteome ID ¹ : UP000002428 GCA_000002545.2 from ENA/EMBL

Chemicals, peptides, and recombinant proteins

Stem cell factors	Cho-SCF	In-house
Recombinant murine stem cell factors	Peptotech	Cat. #: AF-250
Recombinant murine Interleukin-3	Peptotech	Cat. #: 213-13
Recombinant murine Interleukin-6	Peptotech	Cat. #: 216-16
Recombinant human G-CSF	Peptotech	Cat. #: 300-23
Fibronectin human plasma	Sigma	Cat. #: F0895
β -estradiol	Sigma	Cat. #: E2758
Albumin from human serum	Sigma	Cat. #: A9511
4-Aminophthalhydrazide (isoluminol)	Sigma	Cat. #: A8264
Peroxidase from horseradish	Sigma	Cat. #: P6782
PP2	Selleck	Cat. #: S7008
R406	Selleck	Cat. #: S2194
Ibrutinib (PCI-32765)	Selleck	Cat. #: S2680
Cytochrome c from equine heart	Sigma	Cat. #: C7752
Trehalose-6,6-dibehenate (TDB)	Invivogen	Cat # tlr1-tdb CAS number: 66,758-35-8
Furfurman	Invivogen	Cat # tlr1-ffm
Curdlan	Invivogen	Cat # tlr1-curd CAS number: 54,724-00-4
Alexa 488-conjugated fibrinogen	Invitrogen	Cat #F13191

Critical commercial assays

PrestoBlue assay kit	Thermo Fisher	Cat #A13261
----------------------	---------------	-------------

Experimental models: organisms/strains

B6.129S5-Skap2 ^{Gt(VICTR20)21Lex} /Mmjax	Jackson Laboratory	RRID:MGI:4353994
BALB/c	Taconic Laboratory	RRID:IMSR_TAC:balb
BALB/cAnNTac		
C57BL/6J	Jackson Laboratory	RRID:IMSR_JAX:000664
Skap2 ^{-/-} BALB/c	Dr. Kenneth Swanson (Alenghat et al., 2012; Togni et al., 2005)	NA

Recombinant DNA

MSCVneo-HA-ER-Hoxb8	DB Sykes, (Wang et al., 2006)	NA
5676-pMK3B-MSCV-GFP-IRES-PuroR	SC Bunnell, Tufts University	NA

(Continued on next page)

Continued

REAGENT or RESOURCE	SOURCE	IDENTIFIER
5677-pMK3B-MSCV-3xFlag-TRT-IRES-ZeoR	SC Bunnell, Tufts University	NA
Software and algorithms		
FlowJo software v10	Tree Star	FlowJo, RRID:SCR_008520
GraphPad Prism	GraphPad	RRID:SCR_002798
Image Studio lite	Licor	RRID:SCR_013715
ImageJ	Research Services Branch National Institutes of Mental Health	RRID:SCR_003070
Other		
Immunolon 4HBX 96-well plates	Fisher Scientific	Cat. #: 3855
Ficoll-Paque-plus	Pharmacia/GE Healthcare	Cat. #: GE17-1440-02
e-Myco Mycoplasma PCR detection kit	Bulldog Bio	Cat. #: 25,233

RESOURCE AVAILABILITY

Lead contact

Further information and requests for resources and reagents should be directed to and will be fulfilled by the lead contact, Joan Meccas (joan.meccas@tufts.edu), Department of Molecular Biology and Microbiology, School of Medicine, Tufts University, Boston, MA 02111 USA.

Materials availability

Investigators interested in HoxB8 *Skap2*^{-/-} myeloid progenitor cell lines need to submit a Materials Transfer Form to Tufts University. For the ER-HoxB8 construct, a Materials Transfer Form was required from UCSD. C57BL/6j *Skap2*^{-/-} mouse strains are available through Jackson Laboratories. BALB/c *Skap2*^{-/-} mice are available as funding permits from the Lead Contact.

Data and code availability

- All data reported in this paper will be shared by the lead contact upon request.
- This study did not generate/analyze any code.
- Any additional information required to reanalyze the data reported in this paper is available from the lead contact upon request.

EXPERIMENTAL MODEL AND SUBJECT DETAILS

Animals

BALB/c and C57BL/6J mice were purchased from Taconic Biosciences, and Jackson laboratory (Bar Harbor, ME), respectively. Generation of *Skap2*^{-/-} mice in the BALB/c background were a gift of Dr. Kenneth Swanson (Togni et al., 2005; Alenghat et al., 2012). Mating pairs of *Skap2*^{+/-} (B6.129S5-Skap2^{Gt(VICTR20)}^{21Lex}/Mmjax) were purchased from Jackson laboratory and bred in the specific pathogen-free facility of Tufts University. Mouse tail clips from pups were incubated with 10% proteinase K (Viagen Biotech) in lysis buffer (Viagen Biotech) 55°C for 4–5 hr with occasional vortexing; the proteinase K activity was then inactivated by incubating the samples at 85–90°C for 45 min. This solution was used directly for PCR reactions. Two independent PCRs were conducted using Hotstart Taq Mastermix and primer with the following sequences: SkapLeft-forward primer (common for both PCRs), 5' CAG CTT GCC GAC TTT TCT; GTLexVir, 5'GAG GGC TGG ACC GCA TCT GG; GTSkapRight, 5'CCG CCT CCC ACC CCT CAA TC from Jackson laboratory and (Alenghat et al., 2012). Healthy female and male animals aged between 8 and 12 weeks were randomly subjected *K. pneumoniae* infections for analysis of C-type lectin receptors; based on our prior work (Nguyen et al., 2020), there was no difference in experimental results due to sex differences. For neutrophil transfer experiment, randomly selected healthy female wild-type C57BL/6J mice aged

between 8 and 12 were used to gender match with the DIV neutrophils. All mice were handled in accordance with protocols approved by the Institutional Animal Care and Use Committee of Tufts University under the protocol #B2018-10.

Bone marrow neutrophil isolation

Mouse bone marrow (BM) neutrophils were isolated using a three-step Percoll density gradient (55%, 65%, and 75%), and centrifuged at 480 x g for 30 min at 26°C with the break off (Nguyen et al., 2020; Shaban et al., 2020; Rolan et al., 2013). Neutrophils were collected at the 65–75% interface, resuspended in HBSS without Ca²⁺ and Mg²⁺ (HBSS-), and then centrifuged at 250 x g at room temperature (RT). The supernatants were then removed, and the cells were resuspended in HBSS- for a total of three washes. Neutrophils were then rested at RT for one hour, and then centrifuged at 250 x g at RT. The supernatant was removed, and the cells were resuspended in HBSS with Ca²⁺ and Mg²⁺ (HBSS+) to the desired concentration, first incubated at RT for 20 min, then shifted to 37°C for 10 min. The cells are then used for various *in vitro* assays.

HoxB8 cell culture system

ER-HoxB8-carrying granulocyte-monocyte progenitor cells (HoxB8 GMPs) were generated from murine stem cells from female mice (Wang et al., 2006; Nguyen et al., 2020). Murine BM cells were collected, and stem cells were isolated using Ficoll-Paque-Plus (Pharmacia) gradient and immortalized with ER-HoxB8. Briefly, BM cells were centrifuged at 400 x g for 25 min at RT without applying the break to enrich for mononuclear cells. These cells expanded in 6-well tissue culture (TC) plate for 24 hr at 37°C with 5% CO₂ in complete RPMI, cRPMI (RPMI-1640 with 10% FBS, 2mM L-glutamine, and 100U penicillin & 0.1mg/ml streptomycin), supplemented with 10ng/ml stem cell factor (SCF), 10ng/ml interleukin-3 (IL-3), and 10ng/ml interleukin-6 (IL-6). Non-adherent cells were then harvested, centrifuged at 250 x g at RT, resuspended in cRPMI at 1 × 10⁶ cells/ml, and plated onto a 12-well TC plate (Corning) coated with 10μg/ml human fibronectin (Sigma) (500μL/well). The MSCVneo-HA-ER-HoxB8 retroviral supernatant was added along with polybrene (final concentration: 8μg/ml), and the plates were centrifuged at 1000 x g for 90 min at RT. The cells then were maintained in cRPMI supplemented with 0.5 μM beta-estradiol (Sigma, E2) and 5% SCF-conditioned media (SCF + E2 cRPMI; SCF conditioned media was generated from CHO-SCF from David Sykes lab, MGH). The cells were maintained for 3-4 weeks to select for HoxB8 GMPs. Uninfected control cells died by 4 weeks. Isolation, growth and assays with these HoxB8 and bone marrow-derived neutrophils were approved by the Institutional Biosafety Committee at Tufts University protocol number 2017-BR54.

For neutrophil experiments, aliquots of ER-HoxB8 progenitors were washed 3 times in PBS and cultured in cRPMI without E2 media, supplemented with 5% SCF-conditioned media, IL-3, and GCSF for 48 hr (Nguyen et al., 2020; Pelletier et al., 2017). The cells were then restimulated with 50ng/ml GCSF for another 48 hr, unless otherwise indicated. Cells were maintained at a cell concentration of 2.5 × 10⁵ cells/ml throughout the differentiation process. At this point, the cells were differentiated and termed DIV (differentiated *in vitro*) neutrophils. The DIV neutrophils were collected, pelleted at 250 x g for 5 min at 4°C, re-suspended in HBSS-, and then treated as BM neutrophils for functional assays, unless otherwise indicated. DAPI staining and flow cytometry (antibodies described below) were performed to confirm that >90% of cells were neutrophils (Nguyen et al., 2020). The viability was assessed using trypan blue (Gibco) exclusion test prior to functional studies to confirm that >85% of cells are live. SKAP-2 expression in DIV neutrophils was authenticated by generating cell lysates, and probing SKAP-2 expression by Western blot analysis. Mycoplasma testing of cultured cells was conducted regularly (~6 months) using e-Myc Mycoplasma PCR Detection Kit (Bulldog Bio).

Human neutrophil isolation

Human neutrophils from peripheral whole blood were obtained by the Leong lab at Tufts University (Adams et al., 2020). All human cell work were handled in accordance with protocols approved by the Institutional Review Board (IRB) of Tufts Medical Center and Tufts University under protocol #10489, and informed consent was obtained from subjects. Peripheral blood was collected using a 50mL syringe pre-loaded with anticoagulant buffer (13.7 g citric acid, 25 g sodium citrate, and 20g dextrose per liter). Blood was then centrifuge at 2200 rpm for 20 min at room temperature. Supernatant was removed and gelatin (final concentration 2%) was added to the remainder and incubated for 25–60 min at 37°C for gradient separation. Neutrophils were collected at the appropriate layer and centrifuged at 2200 rpm for 10 min at room temperature (RT). Cells were then resuspended in RBC lysis buffer (NH₄Cl, NaHCO₃, and EDTA), RBC lysis

buffer was neutralized with HBSS-, and cells were centrifuged at 1200 rpm for 10 min at 4°C. Supernatant was removed, and cells were washed two more times using HBSS- at 4°C prior to use.

Bacterial and fungal strains

Wild type *C. albicans* (SC5314) and *C. glabrata* (ATCC 2001) were obtained from Michael Mansour lab (MGH, Boston) (Negoro et al., 2020; Xu et al., 2018). Yeast cultures were grown overnight in liquid YPD at 30°C with shaking, washed twice in PBS, counted with the hemocytometer, and resuspended in PBS (Negoro et al., 2020; Xu et al., 2018). MKP220, a streptomycin-resistant, capsule type K2 derivative of *K. pneumoniae* ATCC43816 was grown overnight in liquid LB at 37°C with aeration (Silver et al., 2019; Nguyen et al., 2020; Paczosa et al., 2020). Overnight cultures were used for *in vivo* infections. For *in vitro* experiments, overnight *K. pneumoniae* cultures were diluted 1:40 into LB, and grown for an additional 2 hr at 37°C. The optical density was measured to estimate for colony forming unit (cfu), and the bacteria were resuspended in PBS to the desired inoculum and plated on L-agar to obtain an accurate cfu.

METHOD DETAILS

Flow cytometry

Flow cytometry of antibody staining of surface receptors was conducted by suspending cells in PBS without Ca²⁺ and Mg²⁺ (PBS) containing 1% FBS (FACS buffer), and adding rat anti-mouse CD16/CD32 (Mouse BD Fc Block, BD Biosciences) to block Fc receptors for 10 min at 4°C. Antibodies (final concentration 1:300, unless otherwise indicated) were then added for 30 min at 4°C. Cells were then washed twice with cold FACS buffer, and in some cases resuspended in 100 µl of FACS buffer containing secondary antibody for a further 1 hr at 4°C. Cell staining was analyzed using a BD LSRII, and analyzed using FlowJo software (Tree Star, v10).

The following antibodies were used in experiments to assess the purity of neutrophils. Conjugated antibodies for flow cytometry: α -CD11b (clone M1/70), α -Ly6G (clone:1A8), and α -Gr1(clone: RB6-8C5), α -c-Kit (clone: 2B8), and α -Ly6C (clone: HK1.4). Non-conjugated primary antibodies along with secondary fluorescent antibodies for staining C-type lectin receptors (CLRs): rat α -mouse Dectin-1 (Biolegend, clone: RH1) followed by Alexa 594-conjugated goat anti-rat (Invitrogen), rabbit α -mouse Mincle (MyBioSource) followed by Alexa 594-labeled goat α -rabbit (Invitrogen), or biotinylated goat α -mouse Dectin-2 (R&D Systems) followed by APC-conjugated streptavidin antibodies (Biolegend).

DIV neutrophil *in vivo* transfer experiment

HoxB8 GMPs from female C57BL/6J wild-type or *Skap2*^{-/-} were transduced with MSCV plasmids containing 3xFlag with TRT and zeomycin or with GFP and puromycin from Stephen Bunnell lab (Tufts) to generate fluorescent GMPs. Fluorescent GMPs selected by growing the cells in cultures containing zeomycin or puromycin for 5 or 2 days, respectively. Fluorescence expression was analyzed using flow cytometry. Aliquots of ER-HoxB8 GMP were washed 3 times in PBS and cultured in estrogen-free complete RPMI, cRPMI supplemented with 5% SCF-conditioned media, 10ng/ml IL-3, and 10ng/ml GCSF for four days. On day 4, DIV neutrophils were collected, pelleted at 250 x g for 5 min at 4°C, washed twice with cold sterile PBS, and resuspended in cold sterile PBS at a concentration of 5 × 10⁷ cells/ml. 150 µl of cells or sterile PBS were intravenously injected into mice that had been injected intraperitoneally with 100µL of PBS or 50µg/ml α -Ly6G antibody (clone: 1A8) 16 hr prior (Nguyen et al., 2020). An hour later, mice were retropharyngeally infected with 5 × 10³ cfu of *K. pneumoniae*. Mice were sacrificed after 24 hour and lungs were collected, weighed, and aseptically homogenized using a 70µM cell strainer (Nguyen et al., 2020). Aliquots of cell suspension was serially diluted, plated on L-agar, and incubated at 37°C overnight to assess cfu/g lung. The rest of the homogenates were treated with 1mg/ml Collagenase D (ThermoFisher Scientific) for 1 hr at 37°C, and then with 1X PharmLyse (Fisher Scientific) for 5 min at 4°C. Cells were then suspended in cold FACS buffer and prepared for analysis by flow cytometry as described above. Data were compiled from n = 3 independent experiments with 1–2 mice per group and presented as geometric means with 95% confidence interval. Significance was assessed using one-way ANOVA with Sidak's post-test.

C-type lectin receptors (CLRs) expression

BALB/c wild-type or *Skap2*^{-/-} were intranasally infected with 5 × 10³ colony forming unit (cfu) *K. pneumoniae*, and at 24 hr post-infection, lungs were harvested and were treated as describe above. Cells were then suspended in cold FACS buffer, treated with rat anti-mouse CD16/CD32 (Mouse BD Fc Block, BD

Biosciences) and surface stained for neutrophil markers along with Dectin-1, Mincle or Dectin-2. For intracellular staining, cells were fixed with 4% formaldehyde, permeabilized with 0.1% saponin in FACS buffer (Sigma-Aldrich), and stained with the CLR antibodies in 0.1% saponin/FACS buffer for 30 min at 4°C, followed by the respective secondary antibody in 0.1% saponin/FACS buffer. Data were compiled from $n = 2$ independent experiments with 3 mice each group and presented as geometric means. For CLR staining in DIV neutrophils, aliquots of WT or *Skap2*^{-/-} DIV neutrophils were collected, centrifuged at 250 x *g* for 5 min at 4°C, and resuspended in cold FACS buffer for analysis of CLR as described above. Data were compiled from $n = 5$ –7 independent experiments from two different HoxB8-GMP cell lines, presented as mean + SEM. Data were collected by a BD LSRII, and analyzed using FlowJo software (Tree Star, v10). Significance was assessed using two-tail unpaired Student's *t* test.

Neutrophil ROS assays

High-bound TC 4HBX 96-well plates (Fisher Scientific) were prepared as follows. For C-type lectin (CLR) stimulation, wells were coated with 25µg/ml TDB (InvivoGen), 10µg/ml furfuran (InvivoGen), or 100µg/ml curdlan (InvivoGen) for 3 hr at 37°C and washed once with PBS before use. For controls, cells were plated on wells coated with 10% FBS/PBS, washed twice with PBS prior to use, with or without 100nM of PMA (Nguyen et al., 2020). Cytochrome *c* (Sigma) was added to each well at a final concentration of 100µM for superoxide detection and 1×10^5 neutrophils were added to each well coated with either FBS or CLR ligands (Nguyen et al., 2020; Shaban et al., 2020; Dahlgren et al., 2020). For inhibitor studies, DIV neutrophils were pre-treated with 10nM PP2 (Selleck Chemical), 2µM R406 (Selleck Chemical), 1µM Ibrutinib (Selleck Chemical) or DMSO (1:10,000 final concentration, Sigma) as the vehicle control for 10 min at 37°C with 5% CO₂. To detect ROS production following *Candida* exposure, an isoluminol assay was performed (Kobayashi et al., 2016; Nguyen et al., 2020; Dahlgren et al., 2020). Neutrophils, suspended in HBSS+, were loaded with 50µM isoluminol (Sigma) and 15 units/ml HRP (Sigma), added to a 96-well plate at 1×10^5 cells/well, and incubated at 37°C for 10 min. *C. albicans* and *C. glabrata* were added to wells containing neutrophils at an MOI of 1, and the plate was centrifuged at 500 x *g* for 3 min at 4°C. A BioTek Synergy HT plate reader was used to detect absorbances at 490nm and 550nm for cytochrome *c* assays, or chemiluminescence (RLU) for isoluminol assays. RLU values shown are after subtracting the uninfected samples. Total ROS production was calculated by the sum of the area under the curves for the indicated time in figure legends. Each experiment was conducted in technical triplicates, with representative figure presented as mean ± SD. Unless otherwise indicated, data were compiled from $n \geq 3$ independent experiments, presented as mean ± SEM, and assessed using two-way ANOVA with Tukey's or Sidak's post-test as indicated in the figure legend.

Spreading/adhesion assay

DIV neutrophils (1×10^5 cells/100µL/well) in HBSS+ were plated onto 96-well 4HBX plates coated with 10% FBS, 25µg/ml TDB, 10µg/ml furfuran, 100µg/ml curdlan, or immobilized IgG immune complexes (IC) in technical duplicates, and the plate was spun at 250 x *g* for 2 min. For IC, the wells were coated with 20µg/ml human serum albumin (Sigma) for 1 hr, washed twice with PBS, blocked with 10% FBS for 30 min, washed twice with PBS, and incubated with anti-human serum albumin (Sigma) at 1:400 dilution for 1 hour at 37°C (Jakus et al., 2008; Nguyen et al., 2020). Wells were washed twice prior to use. Cells were incubated at 37°C in presence of 5% CO₂ for 1 hr. The cells were washed twice with RT PBS, and fixed with 4% formaldehyde for 15 min at RT, washed with 200µL of sterile PBS, and then the plate was covered with parafilm and stored at 4°C. The cells were imaged using a Keyence digital bright-field microscope at 20× magnification, and the images were blinded, and assessed for the number of non-spread and spread cells using ImageJ with Fiji. Three random images were taken, and at least 200 cells were counted per well. The percent of adhesion was calculated as follows: (number of spreading cells)/total number of cells counted for each replicate; an average of technical replicates was calculated for each experiment and normalized to the unstimulated level. The average of TDB, furfuran, or curdlan-stimulated total adhesion was then divided by the average IC-stimulated adhesion within the respective experiment. Data were compiled from $n = 3$ –4 independent experiments in technical duplicates, and significance was assessed using one-way or two-way ANOVA with Sidak's post-test as indicated in the figure legend.

Integrin activation

DIV neutrophils (1×10^5 cells/well) in HBSS+ were plated onto 96-well 4HBX plates coated with 10% FBS, 25µg/ml TDB, 10µg/ml furfuran, or 100µg/ml curdlan and the plate was spun at 250 x *g* for 2 min. Negative controls were treated with 2.5mM EDTA for 30 min at 37°C and plated in wells coated with 10% FBS. Cells were incubated at 37°C in the presence of 5% CO₂ for 20 min. 30 µg/mL Alexa 488-conjugated fibrinogen (Invitrogen) was added to the wells, and the cells were incubated at 37°C in presence of 5% CO₂ for an additional 20 min. In

some FBS-coated wells, 2.5mM manganese (Mn^{2+}) was added to cells for the last 15 min of incubation. Following stimulation, the supernatants were removed, and the wells were washed twice with cold PBS. 200 μ L of cold 2.5 mM EDTA in PBS without Ca^{2+} and Mg^{2+} was then added to each well. The cells were incubated at 4°C for an hour to promote lifting of the cells and transferred into 5 mL FACS tubes with 1% formaldehyde. The FACS tubes were covered with paraffin, and stored in the dark, at 4°C until flow cytometry analysis. The percentage of fibrinogen positive cells were normalized to EDTA-treated level and presented as a percentage of Mn^{2+} -treated level. Data were compiled from $n = 4-5$ independent experiments in technical duplicate, presented as mean \pm SEM, and assessed using two-way ANOVA with Sidak's post-test.

Neutrophil killing of *Candida*

The PrestoBlue assay kit (Thermo Fisher) was used to measure fungal viability following co-culture with WT and *Skap2*^{-/-} DIV neutrophils. DIV neutrophils in cRPMI were plated in triplicate 96-well non-TC treated plates at a density of 1×10^5 cells/well. WT and *Skap2*^{-/-} DIV neutrophils were stimulated with *C. albicans* or *C. glabrata* (MOI of 0.2) at 37°C in the presence of 5% CO₂ for 2 or 18 hr for *C. albicans* and *C. glabrata*, respectively. Then, the cells were lysed with NP-40. The lysates were incubated with 10% PrestoBlue Cell Viability Reagent in fresh cRPMI for the *C. albicans*, or YPD broth *C. glabrata* (Tam et al., 2019; Xu et al., 2018; Negoro et al., 2020). Fluorescence readings at 560/590nm using a SpectraMax i3x reader (Molecular Devices) or BioTek Synergy H1 at 30°C for at least 18 hr were recorded. PrestoBlue outgrowth data was assessed using GraphPad PRISM 7 nonlinear curve fit equation. Controls included in each plate were media only wells and a standard of *C. albicans* or *C. glabrata* (no neutrophils). Data from the *Candida*-only wells were fitted to linear regression curve and used to calculate the number of surviving yeasts that were co-incubated with or without neutrophils. Percent of yeast killing was calculated as follows: $100 - (100 \times \text{viability of yeast plus neutrophils} / \text{viability of yeast only})$. Data were compiled from $n = 5-6$ independent experiments in technical triplicate, presented as mean \pm SEM, and significance was assessed using appropriate test as indicated in the figure legends.

Western blot analysis

For purified agonists, 7.5×10^5 cells/well in HBSS + DIV neutrophils were plated onto 96-well 4HBX plates coated with IC, 25 μ g/mL TDB, 10 μ g/mL furfuran, or 250 μ g/mL curdlan. DIV neutrophils (7.5×10^5 cells/well) in HBSS+ were plated onto 96-well 4HBX plates coated with 10% FBS. *C. albicans* and *C. glabrata* were added at MOI 2, while *K. pneumoniae* was added at a MOI of 40; the plate was spun at 250 x g for 2 min. The cells were incubated at 37°C in the presence of 5% CO₂ for 15 min, lysed in 1X Novex buffer and $5-7.5 \times 10^5$ cells equivalents were resolved on 4–12% NuPAGE gel (Invitrogen) in MOPS buffer (Nguyen et al., 2020; Shaban et al., 2020). All antibodies were purchased from Cell Signaling Technology and used at a dilution of 1:1000, unless otherwise indicated. Antibodies to phosphorylated proteins include Syk-Y352, Pyk2-Y402, ERK1/2-Thr202/Tyr204, and pp38-Thr180/Y182. All blots were also probed with RhoGDI. Secondary LI-COR goat anti-mouse or goat anti-rabbit IR-Dye 800 CW were used at a dilution of 1:20,000. The blots were then stripped with 7M Guanidine Hydrochloride (Fisher Scientific) at 56°C for 30 min shaking, washed 3 times in 1x TBST (0.1% Tween 20 in 1x TBS) (Nguyen et al., 2020; Shaban et al., 2020), and re-probed with antibodies for total proteins against Syk, Pyk2, ERK1/2, and p38. The Odyssey CLx LI-COR system and IS Image Studio Lite were used for analysis of the blots and quantification of bands. For CLR and *K. pneumoniae*-stimulated samples, the normalized protein level of pp38 were calculated by taking the ratio of phosphorylated protein to RhoGDI loading control. For all other samples, the normalized protein levels of pSyk, pPyk2, pERK1/2 and p38 were calculated as described in Tables S1–S9. The relative induction of phosphorylation in the unstimulated controls was determined by dividing the fold change of each experiment by the average of the three experiments. Values for fold-change were log transformed, except for *C. albicans* and *C. glabrata*-stimulated pPyk2, and subjected to statistical analysis as indicated in the figure legends. Data were compiled from $n = 3-5$ independent experiments, and unless otherwise indicated, presented as mean \pm SEM.

QUANTIFICATION AND STATISTICAL ANALYSIS

For pooled data from independent experiments, the mean and SEM of each group were calculated for all experiments. For representative data in technical replicates, the mean and SD of each group were

calculated. For data from *in vivo* infections, center bars are geometric means with 95% confidence interval calculated. The number of samples is indicated in the figure legends and [STAR Methods](#). Flow cytometry, imaging, and Western blot data were analyzed using FlowJo (v10), ImageJ with Fiji, or Odyssey CLx LICOR system and IS Image Studio Lite, respectively, as indicated in the [STAR Methods](#). Student's t tests or ANOVA tests were performed using PRISM 7 (GraphPad), with p values indicated in the figures and the appropriate tests indicated in the figure legends and/or [STAR Methods](#).